A UNITED STATES DEPARTMENT OF COMMERCE PUBLICATION

NBS SPECIAL PUBLICATION 260-28

Standard Reference Materials:

PREPARATION AND EVALUATION OF SRM'S 481 AND 482 GOLD-SILVER AND GOLD-COPPER ALLOYS FOR MICROANALYSIS

U.S. DEPARTMENT OF COMMERCE
National Bureau of Standards

NATIONAL BUREAU OF STANDARDS

The National Bureau of Standards[1] was established by an act of Congress March 3, 1901. The Bureau's overall goal is to strengthen and advance the Nation's science and technology and facilitate their effective application for public benefit. To this end, the Bureau conducts research and provides: (1) a basis for the Nation's physical measurement system, (2) scientific and technological services for industry and government, (3) a technical basis for equity in trade, and (4) technical services to promote public safety. The Bureau consists of the Institute for Basic Standards, the Institute for Materials Research, the Institute for Applied Technology, the Center for Computer Sciences and Technology, and the Office for Information Programs.

THE INSTITUTE FOR BASIC STANDARDS provides the central basis within the United States of a complete and consistent system of physical measurement; coordinates that system with measurement systems of other nations; and furnishes essential services leading to accurate and uniform physical measurements throughout the Nation's scientific community, industry, and commerce. The Institute consists of a Center for Radiation Research, an Office of Measurement Services and the following divisions:

Applied Mathematics—Electricity—Heat—Mechanics—Optical Physics—Linac Radiation[2]—Nuclear Radiation[2]—Applied Radiation[2]—Quantum Electronics[3]—Electromagnetics[3]—Time and Frequency[3]—Laboratory Astrophysics[3]—Cryogenics[3].

THE INSTITUTE FOR MATERIALS RESEARCH conducts materials research leading to improved methods of measurement, standards, and data on the properties of well-characterized materials needed by industry, commerce, educational institutions, and Government; provides advisory and research services to other Government agencies; and develops, produces, and distributes standard reference materials. The Institute consists of the Office of Standard Reference Materials and the following divisions:

Analytical Chemistry—Polymers—Metallurgy—Inorganic Materials—Reactor Radiation—Physical Chemistry.

THE INSTITUTE FOR APPLIED TECHNOLOGY provides technical services to promote the use of available technology and to facilitate technological innovation in industry and Government; cooperates with public and private organizations leading to the development of technological standards (including mandatory safety standards), codes and methods of test; and provides technical advice and services to Government agencies upon request. The Institute also monitors NBS engineering standards activities and provides liaison between NBS and national and international engineering standards bodies. The Institute consists of the following technical divisions and offices:

Engineering Standards Services—Weights and Measures—Flammable Fabrics—Invention and Innovation—Vehicle Systems Research—Product Evaluation Technology—Building Research—Electronic Technology—Technical Analysis—Measurement Engineering.

THE CENTER FOR COMPUTER SCIENCES AND TECHNOLOGY conducts research and provides technical services designed to aid Government agencies in improving cost effectiveness in the conduct of their programs through the selection, acquisition, and effective utilization of automatic data processing equipment; and serves as the principal focus within the executive branch for the development of Federal standards for automatic data processing equipment, techniques, and computer languages. The Center consists of the following offices and divisions:

Information Processing Standards—Computer Information—Computer Services—Systems Development—Information Processing Technology.

THE OFFICE FOR INFORMATION PROGRAMS promotes optimum dissemination and accessibility of scientific information generated within NBS and other agencies of the Federal Government; promotes the development of the National Standard Reference Data System and a system of information analysis centers dealing with the broader aspects of the National Measurement System; provides appropriate services to ensure that the NBS staff has optimum accessibility to the scientific information of the world, and directs the public information activities of the Bureau. The Office consists of the following organizational units:

Office of Standard Reference Data—Office of Technical Information and Publications—Library—Office of Public Information—Office of International Relations.

---

[1] Headquarters and Laboratories at Gaithersburg, Maryland, unless otherwise noted; mailing address Washington, D.C. 20234.
[2] Part of the Center for Radiation Research.
[3] Located at Boulder, Colorado 80302.

UNITED STATES DEPARTMENT OF COMMERCE • Maurice H. Stans, *Secretary*
NATIONAL BUREAU OF STANDARDS • Lewis M. Branscomb, *Director*

Standard Reference Materials:

Preparation and Evaluation of SRM's 481 and 482 Gold-Silver and Gold-Copper Alloys for Microanalysis

Kurt F. J. Heinrich, Robert L. Myklebust,
Stanley D. Rasberry,

Analytical Chemistry Division

and

Robert E. Michaelis

Office of Standard Reference Materials

Institute for Materials Research
National Bureau of Standards
Washington, D.C. 20234

National Bureau of Standards Special Publication 260-28

Nat. Bur. Stand. U.S. , Spec. Publ. 260.28, pages (August 1971)

CODEN: XNBSA

Issued August 1971

PREFACE

Standard Reference Materials (SRM's) as defined by the National Bureau of Standards are "well-characterized materials, produced in quantity, that calibrate a measurement system to assure compatibility of measurement in the nation." SRM's are widely used as primary standards in many diverse fields in science, industry, and technology, both within the United States and throughout the world. In many industries traceability of their quality control process to the national measurement system is carried out through the mechanism and use of SRM's. For many of the nation's scientists and technologists it is therefore of more than passing interest to know the details of the measurements made at NBS in arriving at the certified values of the SRM's produced. An NBS series of papers, of which this publication is a member, called the NBS Special Publication - 260 Series is reserved for this purpose.

This 260 Series is dedicated to the dissemination of information on all phases of the preparation, measurement, and certification of NBS-SRM's. In general, much more detail will be found in these papers than is generally allowed, or desirable, in scientific journal articles. This enables the user to assess the validity and accuracy of the measurement processes employed, to judge the statistical analysis, and to learn details of techniques and methods utilized for work entailing the greatest care and accuracy. It is also hoped that these papers will provide sufficient additional information not found on the certificate so that new applications in diverse fields not foreseen at the time the SRM was originally issued will be sought and found.

Inquiries concerning the technical content of this paper should be directed to the author(s). Other questions concerned with the availability, delivery, price, and so forth will receive prompt attention from:

Office of Standard Reference Materials
National Bureau of Standards
Washington, D. C. 20234

J. Paul Cali, Chief
Office of Standard Reference Materials

OTHER NBS PUBLICATIONS IN THIS SERIES

NBS Spec. Publ. 260, Catalog of Standard Reference Materials, July 1970. 75 cents.* (Supersedes NBS Misc. Publ. 260, January 1968 and NBS Misc. Publ. 241, March 1962.)

NBS Misc. Publ. 260-1, Standard Reference Materials: Preparation of NBS White Cast Iron Spectrochemical Standards, June 1964. 30 cents.*

NBS Misc. Publ. 260-2, Standard Reference Materials: Preparation of NBS Copper-Base Spectrochemical Standards, October 1964. 35 cents.*

NBS Misc. Publ. 260-3, Standard Reference Materials: Metallographic Characterization of an NBS Spectrometric Low-Alloy Steel Standard, October 1964. 20 cents.*

NBS Misc. Publ. 260-4, Standard Reference Materials: Sources of Information on Standard Reference Materials, February 1965. 20 cents.*

NBS Misc. Publ. 260-5, Standard Reference Materials: Accuracy of Solution X-Ray Spectrometric Analysis of Copper-Base Alloys, March 1965. 25 cents.*

NBS Misc. Publ. 260-6, Standard Reference Materials: Methods for the Chemical Analysis of White Cast Iron Standards, July 1965. 45 cents.*

NBS Misc. Publ. 260-7, Standard Reference Materials: Methods for the Chemical Analysis of NBS Copper-Base Spectrochemical Standards, October 1965. 60 cents.*

NBS Misc. Publ. 260-8, Standard Reference Materials: Analysis of Uranium Concentrates at the National Bureau of Standards, December 1965. 60 cents.*

NBS Misc. Publ. 260-9, Standard Reference Materials: Half Lives of Materials Used in the Preparation of Standard Reference Materials of Nineteen Radioactive Nuclides Issued by the National Bureau of Standards, November 1965. 15 cents.*

NBS Misc. Publ. 260-10, Standard Reference Materials: Homogeneity Characterization on NBS Spectrometric Standards II: Cartridge Brass and Low-Alloy Steel, December 1965. 30 cents.*

NBS Misc. Publ. 260-11, Standard Reference Materials: Viscosity of a Standard Lead-Silica Glass, November 1966. 25 cents.*

NBS Misc. Publ. 260-12, Standard Reference Materials: Homogeneity Characterization of NBS Spectrometric Standards III: White Cast Iron and Stainless Steel Powder Compact, September 1966. 20 cents.*

NBS Misc. Publ. 260-13, Standard Reference Materials: Mössbauer Spectroscopy Standard for the Chemical Shift of Iron Compounds, July 1967. 40 cents.*

NBS Misc. Publ. 260-14, Standard Reference Materials: Determination of Oxygen in Ferrous Materials -- SRM 1090, 1091, and 1092, September 1966. 30 cents.*

NBS Misc. Publ. 260-15, Standard Reference Materials: Recommended Method of Use of Standard Light-Sensitive Paper for Calibrating Carbon Arcs Used in Testing Textiles for Colorfastness to Light, June 1967. 20 cents.*

NBS Spec. Publ. 260-16, Standard Reference Materials: Homogeneity Characterization of NBS Spectrometric Standards IV: Preparation and Microprobe Characterization of W-20% Mo Alloy Fabricated by Powder Metallurgical Methods, January 1969. 35 cents.*

NBS Spec. Publ. 260-17, Standard Reference Materials: Boric Acid; Isotopic and Assay Standard Reference Materials, February 1970. 65 cents.*

NBS Spec. Publ. 260-18, Standard Reference Materials: Calibration of NBS Secondary Standard Magnetic Tape (Computer Amplitude Reference) Using the Reference Tape Amplitude Measurement "Process A", November 1969. 50 cents.*

NBS Spec. Publ. 260-19, Standard Reference Materials: Analysis of Interlaboratory Measurements on the Vapor Pressure of Gold (Certification of Standard Reference Material 745), January 1970. 30 cents.*

NBS Spec. Publ. 260-20, Standard Reference Materials: Preparation and Analysis of Trace Element Glass Standards. (In preparation)

NBS Spec. Publ. 260-21, Standard Reference Materials: Analysis of Interlaboratory Measurements on the Vapor Pressures of Cadmium and Silver, January 1971. 35 cents.*

NBS Spec. Publ. 260-22, Standard Reference Materials: Homogeneity Characterization of Fe-3Si Alloy, February 1971. 35 cents.*

NBS Spec. Publ. 260-23, Standard Reference Materials: Viscosity of a Standard Borosilicate Glass, December 1970. 25 cents.*

NBS Spec. Publ. 260-24, Standard Reference Materials: Comparison of Redox Standards. (In preparation)

NBS Spec. Publ. 260-25, Standard Reference Materials: A Standard Reference Material Containing Nominally Four Percent Austenite, February 1971. 30 cents.*

NBS Spec. Publ. 260-26, Standard Reference Materials: National Bureau of Standards-U.S. Steel Corporation Joint Program for Determining Oxygen and Nitrogen in Steel, February 1971. 50 cents.*

NBS Spec. Publ. 260-27, Standard Reference Materials: Uranium Isotopic Standard Reference Materials, April 1971. $1.25.*

*Send order with remittance to: Superintendent of Documents, U.S. Government Printing Office, Washington, D.C. 20402. Remittance from foreign countries should include an additional one-fourth of the purchase price for postage.

TABLE OF CONTENTS

LIST OF FIGURES

PAGE

LIST OF TABLES

PREPARATION AND EVALUATION OF SRM'S 481 AND 482 GOLD-SILVER AND GOLD-COPPER ALLOYS FOR MICROANALYSIS

Kurt F. J. Heinrich, Robert L. Myklebust
and Stanley D. Rasberry

Analytical Chemistry Division

and

Robert E. Michaelis

Office of Standard Reference Materials

Institute for Materials Research
National Bureau of Standards
Washington, D. C. 20234

The reasoning behind the choice of the systems Au-Ag and Au-Cu for SRM's, and their suggested uses are described. We also report on the preparations of the materials, their chemical analysis, the tests performed to ascertain macroscopic and microscopic homogeneity, and on relative x-ray intensity measurements at various x-ray lines and voltages. A description of the instrumentation (matrix scanner), techniques, and programs employed in the homogeneity studies, as well as tables and graphs of the x-ray intensity measurements, are appended.

Key words: Alloys; corrections; electron probe; homogeneity; matrix scanner; microanalysis; quantitative analysis; standard reference materials; x-ray emission.

1. INTRODUCTION

A. Requirements for Standard Reference Materials

Although the foundations for a theoretical method of calculating correction factors for quantitative electron probe microanalysis were established in 1949 [1][1], tests of this method, performed a few years ago on specimens of known composition, raised considerable question concerning capabilities of the electron probe microanalyzer as a quantitative tool [2-4]. It became quite evident that various practical techniques proposed for calculating the corrections [5-10] were in considerable disagreement and that in many cases all proposed procedures failed to properly correct the experimental data obtained by experienced investigators. The resulting analytical errors frequently exceeded 10% relative. A detailed analysis of these tests [3] suggested that the following potential sources of error may be responsible for these failures:

1. Some of the test specimens of presumably well known composition may have been poorly characterized on a macroscopic scale or be microscopically inhomogeneous.

2. Although the fundamentals of the generation of x-rays by electron excitation are well known, there are uncertainties in parameters and constants - such as the x-ray absorption coefficients - which adversely affect the accuracy of the method. The resulting uncertainties may be particularly large if the instrument conditions have been chosen injudiciously [3, 11-14].

3. Lack of adequate computational facilities has frequently prompted the investigator to use simplified calculation procedures which may also introduce error.

---

[1]Figures in brackets indicate references beginning on p. 38.

In order to improve the accuracy of the correction procedures for electron probe microanalysis, it is thus necessary to obtain carefully prepared, microscopically homogeneous, and chemically analyzed standard materials. The measurement under carefully controlled conditions of x-ray emission intensities from these standards, including all necessary correction calculations [15], will permit an empirical adjustment within the precision of the measurement of those factors which are affected presently by uncertainty. Once these factors have been established, the standard reference materials will enable the analyst to test the accuracy of his measurement technique by comparing the relative x-ray intensities he obtains from such materials with those obtained by other operators under carefully defined operating conditions.

The Standard Reference Materials SRM 481 and 482 were selected, prepared, and tested in such a manner as to satisfy the requirements indicated in Part 2 of this report[2]. SRM 481 consists of a series of gold-silver alloys, and SRM 482 a series of gold-copper alloys, both in nominal steps of 20 weight percent and including the pure metals. We will describe the reasons for choosing these particular alloys, their preparation and their characterization, and we will report the results of some x-ray measurements performed on them (See Appendix 1).

B. Choice of Systems

SRM's 481 and 482 contain the elements of atomic numbers 29, 47, and 79, and therefore represent a good cross-section through the range of higher atomic numbers. For copper,

---

[2] An additional material of this type, SRM 480, which has a nominal composition of W80-Mo20 has been issued. It is described in NBS publication 260-16.

(atomic number 29), the mean excitation potential is relatively well known; for this reason, it was selected as a starting point for the empirical determination of mean excitation potential by Duncumb [16]. The x-ray lines observable within the typical range of electron probe spectrometers are the Cu K and L lines, the Ag L lines, and the Au L and M lines. Hence, all three x-ray series are covered, the observable lines cover a considerable wavelength range, and, for two of the elements, more than one series can be observed (See Table 1).

All measurements are affected by significant atomic number effects (stopping power and backscatter). The Cu L, Ag L, and Au M lines are also subject to strong absorption, particularly at high operating voltages. Fluorescence due to the continuum is significant for the intensity of the Cu K and Au L emissions. The Cu K emission is also enhanced by fluorescence due to the Au L lines.

The choice of these alloy systems was strongly influenced by the fact that very accurate methods for the elemental analysis of such alloys are available. Hence, the macroscopic composition of the standard reference materials can be determined within an insignificantly small margin of error. Furthermore, the alloys, as well as the end members, are good conductors of heat and electricity, and can be polished to satisfactory flatness without much difficulty. The elements of both binary systems are miscible in all proportions and the alloys can be prepared with high homogeneity, as shown in the tests to be described later.

Because of the high homogeneity and well-determined composition, the standards should also be useful for other methods of microanalysis, including laser probe analysis, optical emission spectrometry, and spark source mass spectrometry.

Table 1. X-ray line wavelengths and absorption edge wavelengths

Au-Cu System

Edge	Line	λ (Å)[a]
AuL_I		0.86376
AuL_{II}		0.90259
AuL_{III}		1.0400
	$AuL\beta_1$	1.08353
	$AuL\alpha_1$	1.27640
CuK		1.38059
	$CuK\alpha_1$	1.54056
AuM_I		3.616
AuM_{II}		3.936
AuM_{III}		4.518
AuM_{IV}		5.374
AuM_V		5.584
	$AuM\alpha_1$	5.84[b]
CuL_I		11.27[b]
CuL_{II}		13.014
CuL_{III}		13.288
	$CuL\alpha_1$	13.336
AuN_I		16.27[b]

Au-Ag System

AuL_I		0.86376
AuL_{II}		0.90259
AuL_{III}		1.0400
	$AuL\alpha_1$	1.27640
AgL_I		3.2564
AgL_{II}		3.5164
AuM_I		3.616
AgL_{III}		3.6999
	$AgL\beta_1$	3.93473
AuM_{II}		3.936
	$AgL\alpha_1$	4.15443
AuM_{III}		4.518
AuM_{IV}		5.374
AuM_V		5.584
	$AuM\alpha_1$	5.84[b]
AuN_I		16.27[b]
AgM_I		17.24[b]

[a]Extracted from "X-Ray Wavelengths," J. A. Bearden, U.S. A.E.C. Report NYO-10586 (1964).

[b]Extracted from "The Physics of X-rays," M. A. Blokhin, AEC-tr-4502 (1961).

C. Units for Composition

In this report, composition is expressed in mass fractions. This unit is widely used by microprobe analysts in analogy to k, the x-ray intensity ratio, which is also a fraction. Weight percents are retained in designating the alloys (e.g., Au20-Cu80) and in the reproduction of the certificates in Appendix 2.

2. PREPARATION OF THE STANDARD REFERENCE MATERIALS

In addition to the Au-Ag and Au-Cu systems described in this report, several other systems were initially considered. These included Ag-Cu, Au-Al, Al-Ag, and Al-Cu, all of which contain two-phase regions when prepared under equilibrium conditions. Two alternatives are available for the preparation of such alloys; first, they could be solidified in a non-equilibrium condition which would yield an apparent single-phase. A possible technique for doing this is "splat cooling" of molten drops [17]. Secondly, they could be produced as two-phase alloys, either from the melt or by powder metallurgy, with identification and characterization of one or both phases to be certified. This alternative has a major technical difficulty in obtaining reliable chemical analyses of the separate phases. We selected the simpler, single-phase Au-Ag and Au-Cu binaries to be studied first.

That criterion established for acceptable homogeneity was that maximum variations in composition on both the macro- and micro-scale should not exceed a range of 0.01 (mass-fraction). Preliminary testing at NBS was carried out[3] on the macro-scale by residual resistivity ratios (R_{273}/R_4), and on the macro- and micro-scale by electron probe microanalysis[4].

The pure metals and the four intermediate binary alloys (nominal steps of 0.2) that comprise both the Au-Ag and the Au-Cu system were prepared at Cominco American, Incorporated, Spokane, Washington. Approximately 450 g (1 lb)

---

[3] Electronic characterization was performed at NBS (Boulder, Col.) by R. L. Powell, J. G. Hust, and R. L. Rutter. An introductory treatment of electrical resistivity of metals is given by Charles Kittel in Introduction to Solid State Physics, 3rd Ed., John Wiley and Sons, New York, p. 218 (1966).

[4] Electron probe characterization was performed at NBS (Washington, D. C.) by K. F. J. Heinrich, M. A. Giles, and D. L. Vieth.

lots were made for each final wire using "6-9's grade" (nominal 99.9999% purity) starting materials. Melting, casting, and fabrication techniques were designed to ensure maximum homogeneity and minimum contamination.

Weighed portions of the starting materials were melted and cast into a single ingot, 25 mm (1 in.) in diameter, in a high-purity graphite mold. Following surface preparation of the ingot, numerous swaging and drawing operations were employed to produce wire 0.25 mm (.01 in.) in diameter. This wire was spooled, bagged and shipped to NBS. To achieve clean wire surfaces, the wire was drawn without lubricant. A final etch (and frequently intermediate acid cleaning) was also employed.

The first wire for preliminary homogeneity testing was the Au20-Ag80 alloy. Several cross-sections were examined by electron probe microanalysis and revealed the following: (1) each specimen exhibited an outer layer approximately 30-μm thick having a concentration of gold at least two-fold greater than that found at the center of the wire; and (2) at the center of the wire, the mass fraction of gold differed by more than 0.02 at points within 15 μm of each other. The material was not suitable as a standard for microprobe analysis.

Preliminary testing continued on the three remaining alloys in the Au-Ag systems with the following results:

(1) None of the three exhibited the Au-enriched outer layer.

(2) The Au40-Ag60 alloy was unsatisfactory, in terms of homogeneity over the cross-section, the Au60-Ag40 was marginal, but the Au80-Ag20 was entirely satisfactory.

(3) Electronic characterization for macro-homogeneity agreed closely with the microprobe findings in that the Au80-Ag20 was shown homogeneous to within 0.002; the Au40-Ag60 was found to be ten times less homogeneous.

The Au-enriched outer layer of the Au20-Ag80 was attributed to the preferential removal of Ag in the final etching procedure and this material was returned to Cominco American, Inc. for repreparation omitting the final etching. On retesting, no evidence of an enriched Au outer layer was observed.

Meanwhile, experimentation was conducted to establish a homogenization heat treatment[5]. Success was achieved whereby all the wires were shown to be within 0.01 by microprobe evaluations, and within 0.004 by electronic characterization. The homogenization heat treatment was performed on all but the Au80-Ag20 alloy by placing each lot (coiled on a quartz drum, about 0.3 m in diameter) in a vacuum furnace at 650° C for 8 hours, followed by slow cooling in vacuum.

Preliminary homogeneity testing of the four alloys of the Au-Cu systems revealed no outer-layer problem, but again a homogenization heat treatment was necessary for two of the alloys, Au20-Cu80 and Au40-Cu60. Tests on short length wires indicated the best heat treatment to be 8 hours in a vacuum furnace at 700° C, followed by slow cooling in vacuum. After coiling one of the alloys on the quartz cylinder and performing this heat treatment, it was observed that a flashing of copper had been deposited on the quartz cylinder. Chemical determinations were made to check the possible copper deficiency, but fortunately, no significant difference on the bulk sample was observed. As a precautionary measure, however, the final homogenization heat treatment was altered to two 8-hour soakings at 480° C in a nitrogen atmosphere of 0.02 torr in the vacuum furnace. Each soaking was followed by slow cooling in the furnace. Additionally, the Au-Cu wires were proven satisfactory in terms of preliminary homogeneity.

---

[5]Accomplished by C. W. Gifford and G. E. Hicho (National Bureau of Standards, Institute for Materials Research).

Assay results, residual resistivity ratio measurements and preliminary microprobe results are given in Appendix 3. Final homogeneity studies by electron probe microanalysis are reported in detail in Section 4.

3. CHEMICAL ANALYSIS OF BULK COMPOSITION

Bulk analyses of the Standard Reference Materials SRM 481 and 482 were performed by their manufacturer (Cominco American. Inc.), by the U.S. Bureau of the Mint, and by the Analytical Chemistry Division, National Bureau of Standards.

The results of the bulk analyses are as follows.

SRM 481 wire	Color code	Nominal comp.	Cominco American[a]	U.S. Bureau of the Mint[b]		NBS[c]		Average value[d]	
			Au	Au	Ag	Au	Ag	Au	Ag
			Mass fraction						
A	Gold	Au100	----	----	----	----	----	1.000_0	----
B	Gray	Au80-Ag20	.8000	.8002	.2000	.8013	.1993	$.800_5$	$.199_6$
C	Yellow	Au60-Ag40	.6001	.6011	.3985	.6004	.3998	$.600_5$	$.399_2$
D	Blue	Au40-Ag60	.3999	.4003	.5990	.4006	.5996	$.400_3$	$.599_3$
E	Red	Au20-Ag80	.2242	.2242	.7759	.2246	.7756	$.224_3$	$.775_8$
F	Silver	Ag100	----	----	----	----	----	----	1.000_0

[a]The fire assay method was employed for the determination of Au by Cominco American.

[b]At the U.S. Bureau of the Mint, Au was determined by fire assay and Ag was determined by titration as AgCl.

[c]At NBS, Au was determined from the residue after treatment of the alloys with HNO_3. The Au residue was dissolved in aqua regia, filtered, the Au precipitated by sulfurous acid, and weighed. Ag was determined gravimetrically as AgCl in all four alloys, and also coulometrically in the .8 Ag alloy.

[d]The results of individual laboratories agree within a range of $\pm.001$ from the average values. The agreement between results by the different methods and analysts, and the summation of results close to unity for each binary alloy, indicate that the averages are free from significant bias.

SRM 482 wire	Color code	Nominal comp.	Cominco American[a]	U.S. Bureau of the Mint[b]		NBS[c]		Average value[d]	
			Au	Au	Cu	Au	Cu	Au	Cu
			Mass fraction						
A	Gold	Au100	----	----	----	----	----	1.000_0	----
B	Gray	Au80-Cu20	.8010	.8013	.1981	.8021	.1985	$.801_5$	$.198_3$
C	Blue	Au60-Cu40	.6030	.6037	.3966	.6041	.3962	$.603_6$	$.396_4$
D	Yellow	Au40-Cu60	.4012	.4006	.5988	.4011	.5997	$.401_0$	$.599_2$
E	Red	Au20-Cu80	.2004	.2012	.7984	.2021	.7986	$.201_2$	$.798_5$
F	Copper	Cu100	----	----	----	----	----	----	1.000_0

---

[a]The fire assay method was employed for the determination of Au by Cominco American.

[b]At the U.S. Bureau of the Mint, Au was determined by fire assay and Cu was determined by electrodeposition.

[c]At NBS, Au was determined by precipitation from solution; Cu was determined by electrodeposition.

[d]The results of individual laboratories agree within a range of $\pm$.001 from the average values. The agreement between results by the different methods and analysts, and the summation of results close to unity for each binary alloy, indicate that the averages are free from significant bias.

4. RESULTS OF HOMOGENEITY STUDIES

Each alloy wire was investigated using the electron probe microanalyzer to determine homogeneity along the wire (longitudinal), across the wire (transverse), and on microscopic regions within the wire (micro-). Slices were taken at the two ends and at one to three intermediate positions along each wire. Three transverse specimens from each of the slices were metallographically mounted and polished for the analyses.

Longitudinal homogeneity along individual wires was tested by using 25-μm diameter electron beam at two points located in opposite quadrants of each specimen cross-section. The average of the concentrations obtained from all the slices of each alloy was assumed to be equal to the chemically analyzed concentration. Table 2 lists the average composition of each slice in the Au-Ag system together with its standard deviation. A similar set of data for the Cu-Au system appears in Table 3. Homogeneity along the wires was also tested by measurement of the residual resistivity ratio. These measurements indicated that the variation (macroscopic) of composition along all standard wires was less than 0.001. Further information on longitudinal homogeneity of the wires was obtained by fire assay determinations of Au at the extreme ends of the alloy wire by the Bureau of the Mint; the data also indicate that the extreme variation along the wires is less than 0.001.

For transverse and micro-homogeneity testing, special instrumentation, techniques, and computation procedures were developed. These are described in detail in Appendix 4. Transverse homogeneity was investigated at all slices along the wire; for each slice, measurements were made along two diagonals at right angles. On each diagonal, determinations were made at 25 points, 1 μm or less in diameter, starting and ending at approximately 25 μm from the edge. The variation was calculated in terms of the standard variation for an

individual determination for each traverse. The Au-Ag data are presented in Table 4 and the Au-Cu data in Table 5.

Micro-homogeneity was studied by performing measurements in two-dimensional arrays of 10 x 10 points on each slice. The distance between centers of adjacent points was 3.5 μm. Two arrays were made in opposite quadrants of a specimen from each slice. The observed standard deviations for individual determinations are listed in Table 6 for the Au-Ag system and in Table 7 for the Au-Cu system.

These studies, including those which were not performed with the microprobe, indicate that both sets of SRM's are well within the pre-established goal for homogeneity.

Table 2. Au-Ag Alloys SRM 481
Big-beam determinations of concentrations and standard deviations on homogeneity test slices

Slice[a]		Au20-Ag80		Au40-Ag60		Au60-Ag40		Au80-Ag20	
		Ag	Au	Ag	Au	Ag	Au	Ag	Au
1	C[b]	0.7829	0.2228	0.5992	0.4019	0.4000	0.5972	0.2006	0.8007
	s.d.	.0042	.0057	.0015	.0004	.0026	.0058	.0001	.0018
2	C	.7726	.2249	.6010	.3972	.3972	.6037	.1991	.7966
	s.d.	.0033	.0032	.0025	.0001	.0009	.0020	.0009	.0018
3	C	.7725	.2239	.5985	.4027	.3968	.6045	--	--
	s.d.	.0009	.0004	.0045	.0013	.0006	.0040	--	--
4	C	.7750	.2267	.5988	.3979	.3999	.6016	.1991	.8042
	s.d.	.0011	.0028	.0001	.0031	.0074	.0012	.0016	.0028
5	C	.7761	.2272	.5990	.4018	.4019	.5957	--	--
	s.d.	.0040	.0023	.0019	.0015	.0004	.0011	--	--

[a]Homogeneity test slices are transverse sections selected at widely separated longitudinal test locations. The number scheme for locations along the wire is: 1 - top; 2 through 4 - intermediate; 5 - bottom.

[b]Standard deviations estimated by the range method. See reference 19.

Table 3. Au-Cu Alloys SRM 482
Big-beam determinations of concentrations and standard deviations on homogeneity test slices

Slice[a]		Au20-Cu80		Au40-Cu60		Au60-Cu40		Au80-Cu20	
		Cu	Au	Cu	Au	Cu	Au	Cu	Au
1	C	0.7978	0.1998	0.5972	0.3988	0.3971	0.6056	0.1977	0.7987
	s.d.[b]	.0018	.0008	.0013	.0010	.0005	.0013	.0002	.0013
2	C	.7999	.2022	.5995	.4016	.3959	.6025	.1982	.8027
	s.d.	.0018	.0005	.0017	.0015	.0010	.0014	.0003	.0004
3	C	.7979	.2018	.6010	.4027	.3961	.6028	.1989	.8031
	s.d.	.0005	.0011	.0013	.0012	.0010	.0017	.0003	.0008

[a]Homogeneity test slices are transverse sections selected at widely separated longitudinal test locations. The number scheme for locations along the wire is: 1 - top; 2 - intermediate; 3 - bottom.

[b]Standard deviations estimated by the range method. See reference 19.

Table 4. Au-Ag Alloys
Standard deviations for traverses

Slice[a]	Au20-Ag80		Au40-Ag60		Au60-Ag40		Au80-Ag20	
	Ag	Au	Ag	Au	Ag	Au	Ag	Au
1.								
a.	0.0067	0.0024	0.0020	0.0011	0.0018	0.0010	--	--
b.	.0034	.0012	.0026	.0013	.0021	.0013	.0009	.0020
2.								
a.	.013	.0036	.0016	.0013	.0021	.0016	.0011	.0015
b.	.036	.0032	.0021	.0013	.0017	.0012	.0008	.0018
3.								
a.	.0059	.0012	.0014	.0011	.0016	.0014	--	--
b.	.0046	.0014	.0013	.0008	.0022	.0011	--	--
4.								
a.	.0089	.0037	--	--	.0024	.0008	.0008	.0012
b.	.0070	.0026	--	--	.0019	.0011	.0011	.0022
5.								
a.	.0086	.0039	--	--	.0019	.0011	--	--
b.	.0058	.0027	--	--	.0020	.0015	--	--

[a]Homogeneity slices are transverse sections selected at widely separated longitudinal test locations. The number scheme for locations along the wire is: 1 - top; 2 through 4 - intermediate; 5 - bottom. a. is the average of diagonals in one direction on each slice and b. is the average of diagonals perpendicular to a.

Table 5. Au-Cu Alloys
Standard deviations for traverses

Slice[a]	Au20-Cu80		Au40-Cu60		Au60-Cu40		Au80-Cu20	
	Cu	Au	Cu	Au	Cu	Au	Cu	Au
1.								
a.	0.0024	0.0018	0.0018	0.0013	0.0018	0.0028	0.0012	0.0039
b.	.0044	.0017	.0031	.0023	.0025	.0033	.0009	.0037
2.								
a.	.0029	.0016	.0014	.0015	.0016	.0019	.0013	.0034
b.	.0024	.0013	.0015	.0013	.0027	.0043	.0010	.0044
3.								
a.	(.0099)†	(.0070)†	.0017	.0018	.0018	.0023	.0024	.0064
b.	.0027	.0020	.0014	.0013	.0026	.0051	.0021	.0043

[a]Homogeneity slices are transverse sections selected at widely separated longitudinal test locations. The number scheme for locations along the wire is: 1 - top; 2 - intermediate; 3 - bottom. a. is the average of diagonals in one direction on each slice and b. is the average of diagonals perpendicular to a.

†Set deleted - smear on sample surface covering five of the analysis points.

Table 6. Au-Ag Alloys
Standard deviations for rasters

Slice[a]	Au20-Ag80		Au40-Ag60		Au60-Ag40		Au80-Ag20	
	Ag	Au	Ag	Au	Ag	Au	Ag	Au
1.								
a.	0.0093	0.0023	0.011	0.0019	0.0076	0.0037	0.0011	0.0030
b.	--	--	.012	.0012	.0078	.0057	.0012	.0030
c.	--	--	--	--	.0023	.0019	--	--
2.								
a.	.0063	.0022	.012	.0011	.0070	.0026	.0015	.0031
b.	--	--	.011	.0027	.0070	.0028	.0009	.0025
c.	--	--	--	--	.0027	.0022	--	--
3.								
a.	.0093	.0019	.011	.0015	.0064	.0018	--	--
b.	--	--	--	--	.0066	.0020	--	--
4.								
a.	.0066	.0025	.011	.0018	.0074	.0022	.0011	.0023
b.	--	--	.011	.0017	.0073	.0045	.0010	.0026
c.	--	--	--	--	.0021	.0022	--	--
5.								
a.	.013	.0034	.013	.0012	--	--	--	--

[a]Homogeneity slices are transverse sections selected at widely separated longitudinal test locations. The number scheme for locations along the wire is: 1 - top; 2 through 4 - intermediate; 5 - bottom. a. is the standard deviation for one matrix and b. is

4 - intermediate; 5 - bottom. a. is the standard deviation for one matrix and b. is the standard deviation for the matrix in the opposite quadrant. c. measurements are made in a third quadrant.

Table 7. Au-Cu Alloys
Standard deviations for rasters

Slice[a]		Au20-Cu80		Au40-Cu60		Au60-Cu40		Au80-Cu20	
		Cu	Au	Cu	Au	Cu	Au	Cu	Au
1.									
	a.	0.0059	0.0012	0.0045	0.0030	0.0037	0.0042	0.0022	0.0064
	b.	.0058	.0013	.0048	.0027	.0031	.0030	.0028	.0088
2.									
	a.	.0063	.0019	.0055	.0027	.0034	.0058	.0024	.0076
	b.	.0064	.0020	.0058	.0025	.0031	.0050	.0019	.0057
3.									
	a.	.0080	.0013	.0050	.0026	.0029	.0039	.0026	.0069
	b.	.0078	.0014	.0042	.0031	.0028	.0039	.0024	.0067

[a]Homogeneity slices are transverse sections selected at widely separated longitudinal test locations. The number scheme for locations along the wire is: 1 - top; 2 - intermediate; 3 - bottom. a. is the standard deviation for one matrix and b. is the standard deviation for the matrix in the opposite quadrant.

5. ANALYTICAL MEASUREMENTS WITH THE ELECTRON PROBE ON SRM'S 481 AND 482

Several operators performed measurements of x-ray intensity ratios using the standard reference materials mentioned above. Further measurements are still in progress; therefore, the results presented here should not be considered final. However, they will serve to illustrate the information which can be obtained from these standards and some of the difficulties which present themselves in the process.

A. General Observations

The standards, in the form of cleaned wires, were mounted by press-fitting them into holes drilled into blocks of aluminum or brass. The assembly was then backed by epoxy resin to hold the wires firmly in place, and the cross-sections at the surface of the mounting blocks were carefully polished, finishing with 1/4-μm diamond paste. Since no nonconductive material appeared at the specimen surface, it was not necessary to coat the specimens.

The high voltage power supplies used in these measurements were calibrated by observing the minimum nominal voltage of excitation of selected lines. Therefore, the potential difference between the filament and the negative side of the bias resistor was eliminated as a source of error. The pulse-height analyzers of each channel were used in the discriminator mode, and the amplification of the linear amplifiers was carefully adjusted so that the peak of the pulse-height distribution was five times the height of the discrimination level. The dead time of each channel had been carefully measured as described elsewhere [18]; dead time was about 3 μsec.

The size of the beam cross-section was enlarged to 3-5 μm in order to reduce the effects of contamination, and each measurement was performed at a site which had not been exposed

previously. The specimen remained in a fixed position during the exposures.

Before initiating measurements, the filament was allowed to emit for at least 30 minutes, in order to assure stability of electron emission. The electron optics were realigned before each set of measurements by readjusting the anode plate to maximum target current.

The measurements were performed on scalers by accumulating the number of pulses obtained from each specimen within a fixed time period. Within each set of measurements, each alloy was measured at least twice. The end-member elements were read at the beginning and the end of each set. (This, in fact, defines the limits of a set of measurements.) If the measurements on the pure elements emitting the line in question differed by one percent or more, the series of measurements was rejected. If the measurements of the binary alloys differed among themselves by more than one percent of the readings of the corresponding end member, more measurements were performed within the corresponding set of measurements.

Wherever possible, several lines were measured in the same operation. However, the beam intensity was adjusted in each case to limit the counting rates to a maximum of 15,000 counts/sec. When, under these conditions, another set measured simultaneously showed excessive counting error, this set was rejected and rerun at a larger beam current.

1. Background Correction

In most series, the background was assumed to be equal to the measurement on the end member not containing the emitting element. This practice is open to the objection that the background intensity - which consists mainly of the continuum contribution - increases with increasing atomic number. However, if the background increases or decreases

proportionally to the variation of the line emission, the resulting error cancels. Experimental measurements of background variation as a function of composition (Figure 1) indicate that the background varies nearly linearly with composition. Therefore, the resulting error should be small, as long as the analytical calibration curve is close to linear. Strong deviation from linearity occurs mainly in the case of strong absorption corrections. These are observed only for lines of long wavelength for which the line-to-background ratio is fairly large (>100). It can thus be expected that the errors resulting from the proposed background correction technique for binary alloys will be negligible. This proposition was tested for three cases by determining the background in the proposed manner, as well as by actually measuring the background intensity close to the observed line. The results obtained (Table 8) indicate that the results of both procedures are identical within the accuracy of the measurement.

The advantages accruing from the simplicity of this background correction procedure are obvious. When it is applied to soft x-ray lines, and when low concentrations are measured, it is important to avoid superficial contamination of the background standard - such as smearing effects on a gold surface, particularly if the standards are mounted in brass. Extension of this technique to systems other than metal binaries will be described in a future publication.

2. Consistency Test on Experimental Intensity Ratios

Since the purpose of the measurement of intensity ratios (henceforth called k) is to test theoretical correction procedures, it would not be possible to test the accuracy of the measurements used in calculating k by comparing the experimental results with theoretical predictions. It can be safely assumed, however, that for a given line and operating voltages, the k values within a binary system will

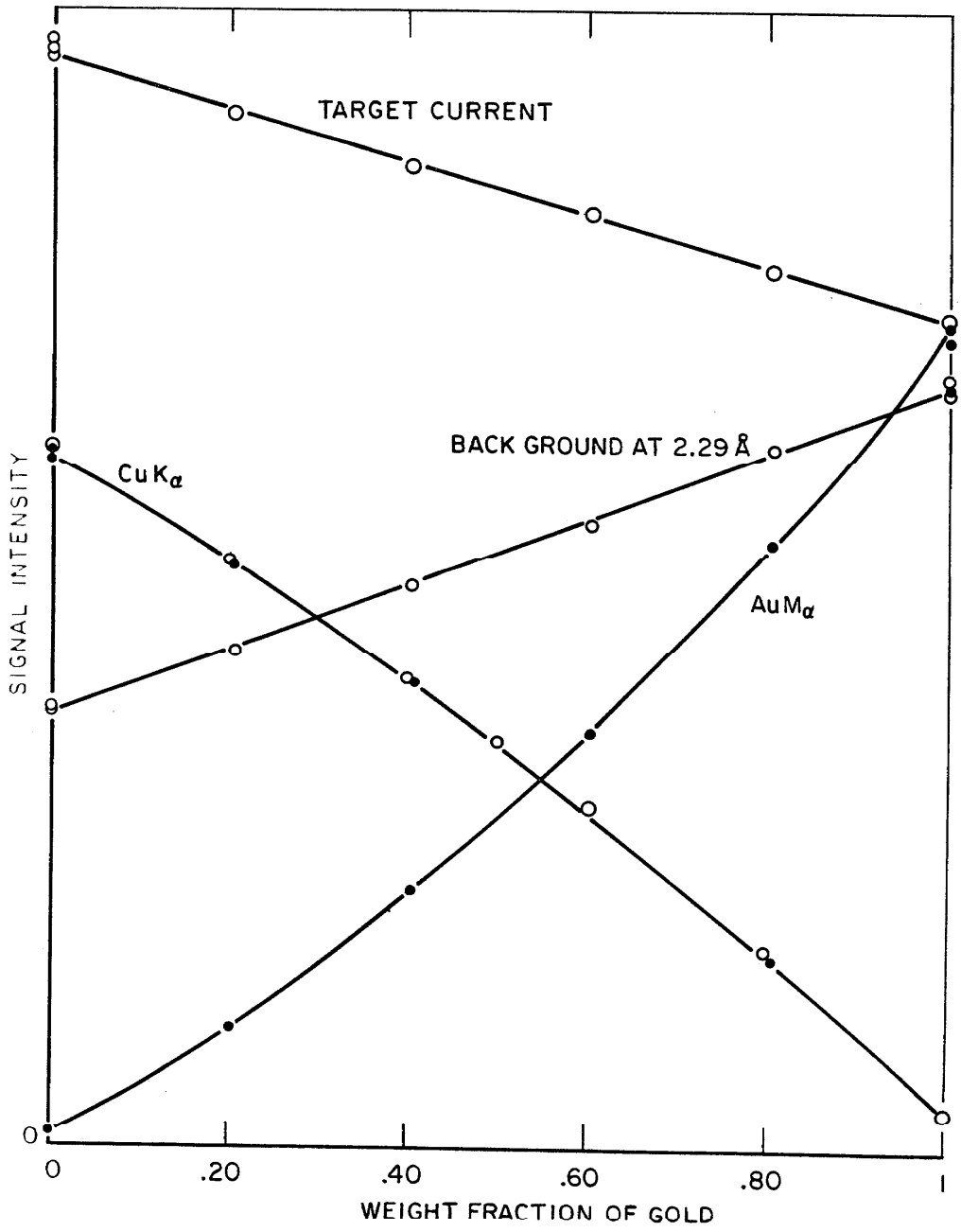

Figure 1. Measurements at 20 kV on copper-gold standard reference materials. The signal intensities are on an arbitrary scale. Both target current and continuous radiation (background at 2.29 Å) vary linearly with mass fraction.

Table 8. Comparison of background-determining methods on Au-Cu alloys

	k					
	AuMα		CuKα		CuLα	
Alloy	Cu[a]	Off-peak[b]	Au[a]	Off-peak	Au[a]	Off-peak
Au80-Cu20	0.7297	0.7297	0.2476	0.2500	0.1091	0.1114
Au60-Cu40	.5030	.5034	.4626	.4643	.2471	.2491
Au40-Cu60	.3065	.3072	.6648	.6657	.4311	.4327
Au20-Cu80	.1407	.1413	.8426	.8429	.6738	.6751

[a]The backgrounds for these k-values were measured on the pure element indicated and assumed to be constant for all the alloys.

[b]The backgrounds for the k-values were determined by measuring intensities at points 0.04 A above and below each peak on each alloy and standard. Individual backgrounds were then calculated by averaging the data above and below each measured x-ray line.

vary smoothly with the weight fraction of the measured element, C, converging to zero as C tends to zero, and to unity as C tends to one. Hence, a plot of experimental k values as a function of C (analytical calibration curve) must give a smooth curve with the end points (0,0) and (1,1). However, small deviations from smoothness are not easily apparent on such a plot. It is therefore preferable to use a simple transformation, plotting the ratio k/C as a function of k, (or the ratio C/k as a function of C). In such a plot, the vertical scale (k/C) can be expanded to any desirable degree so that small irregularities of the calibration curve become more apparent (see Figure 2 and 3).

It is interesting to observe that the hyperbolic approximation of Ziebold and Ogilvie [8] postulates that the plots of k/C vs. k and C/k vs. C yield straight lines. The proposed plot is therefore also a test of this approximation.

Deviations from smoothness of the k/C plot indicate an error in either the measured k value or the assumed composition (C). If the assumed composition is in error, a similar deviation will result on all measurements of the element in question in the standard, regardless of the line and operating voltage used. Furthermore, in a binary alloy, the complementary element would exhibit a comparable deviation in the opposite direction since the sum of C of both elements is equal to unity. On the other hand, errors in individual measurements will not produce similar correlations. An inspection of the curves obtained from the standard reference series (Figures 5 to 13) indicates no such correlations. One must conclude that any irregularities observed in the plots are results of measurement errors. One may not, however, conclude that conversely a smooth k/C curve is proof of correct chemical analysis, since systematic errors in the chemical analysis could produce a smooth shift of the k/C curve.

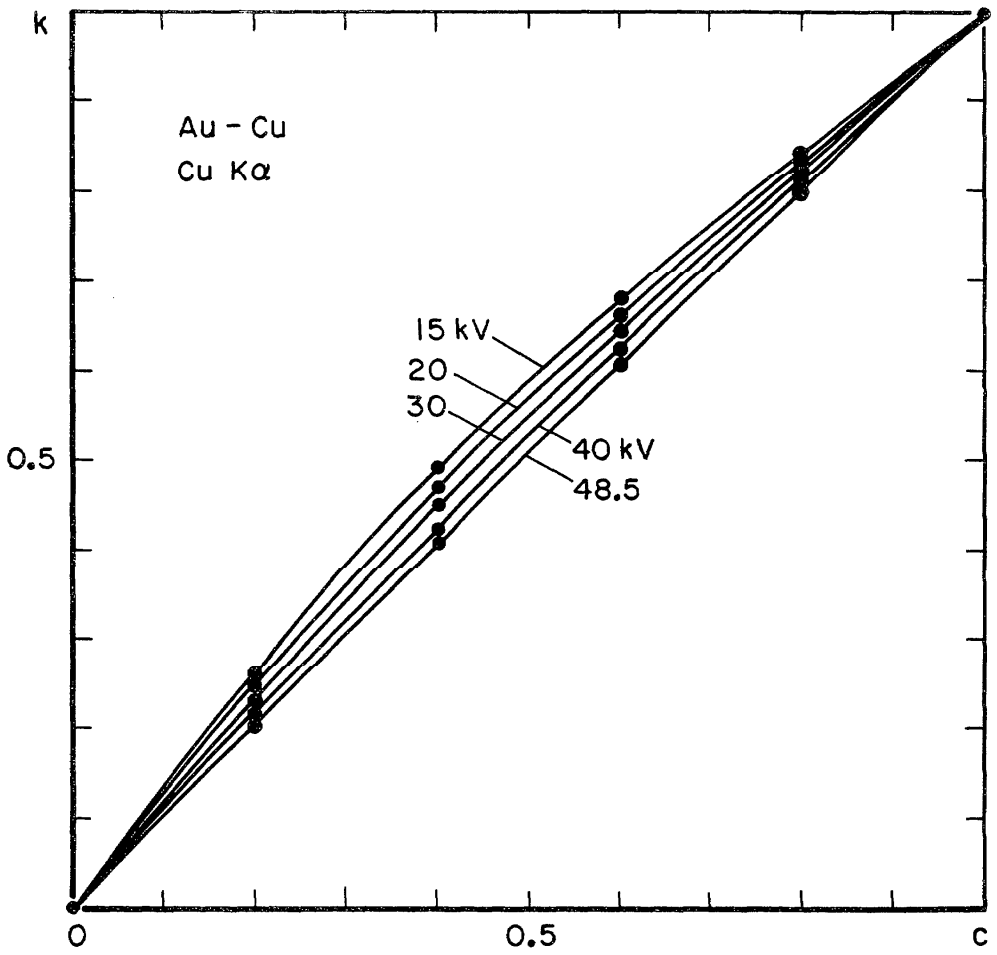

Figure 2. Analytical calibration curves for the copper Kα line in gold-copper binaries at various operating voltages. Background-corrected intensity ratios, k, are plotted vertically and mass fractions of copper, C, horizontally.

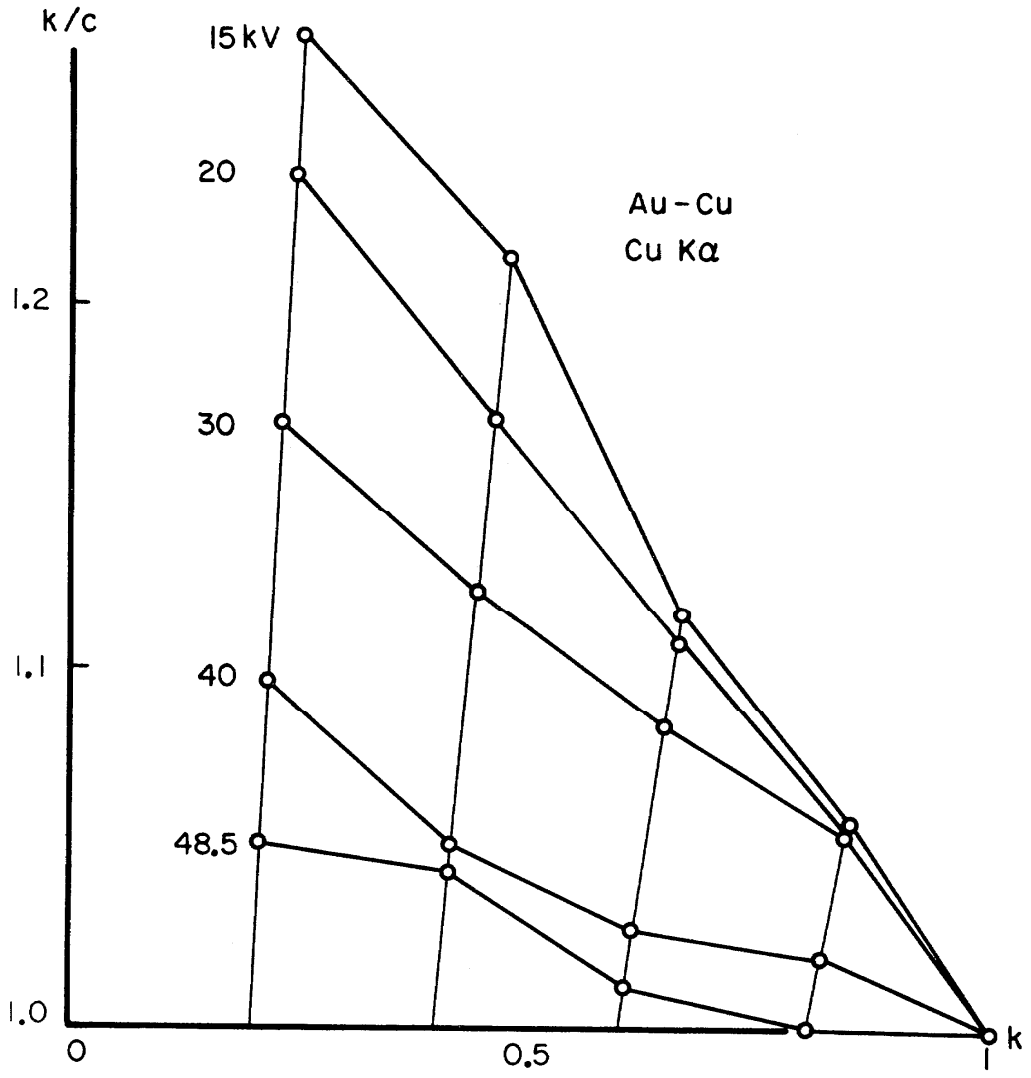

Figure 3. The same measurements as shown in Figure 2 are represented by plotting the ratio k/C on the ordinate, and k on the abscissa. The ordinate scale can be expanded to any degree; therefore, the scatter of experimental data is easier to observe than in Figure 2. The thin, almost vertical lines connect points corresponding to the same composition, which can be read on the horizontal scale, where k = C.

If the measurements of all alloys of a binary system for a line and operating voltage were made in the same set or sets of measurements (as in our study), an error in standardization, or in the assumed operating voltage, could smoothly shift the k/C curve. Such systematic errors are not very obvious on the k/C plots. However, it can also be safely assumed that, above the minimum excitation potential, the values of k must shift smoothly as a function of accelerating voltage. A test for errors affecting a whole series of measurements can thus be performed by plotting the value of k (or of k/C) as a function of accelerating voltage for each alloy. In the absence of measurement errors, a smooth curve should be obtained. One may plot on the same graph the k values predicted by various theoretical procedures; thus, the accuracy of the procedures can also be tested (Figure 4). Alternatively, one may plot the analytical error (i.e., the difference between the assumed C and the value of C obtained from the experimental k, by means of various theoretical procedures). In absence of measurement errors, the obtained curves should also be smooth.

B. Data Obtained

The x-ray intensity measurements presented in this section consist of a preliminary set of data (obtained by operator 1) and some complementary measurements (operator 2 and 3). Since all these measurements were exploratory, in many instances their precision is inferior to that which we ultimately hope to attain. Nevertheless, the data provide very interesting information.

The results are presented in the following form:

1. A table for each element and SRM set gives the mean intensity ratios, k, as well as estimates of the standard deviation of a single measurement, where available (Tables 9 to 12, Appendix 1). The estimates were derived from the

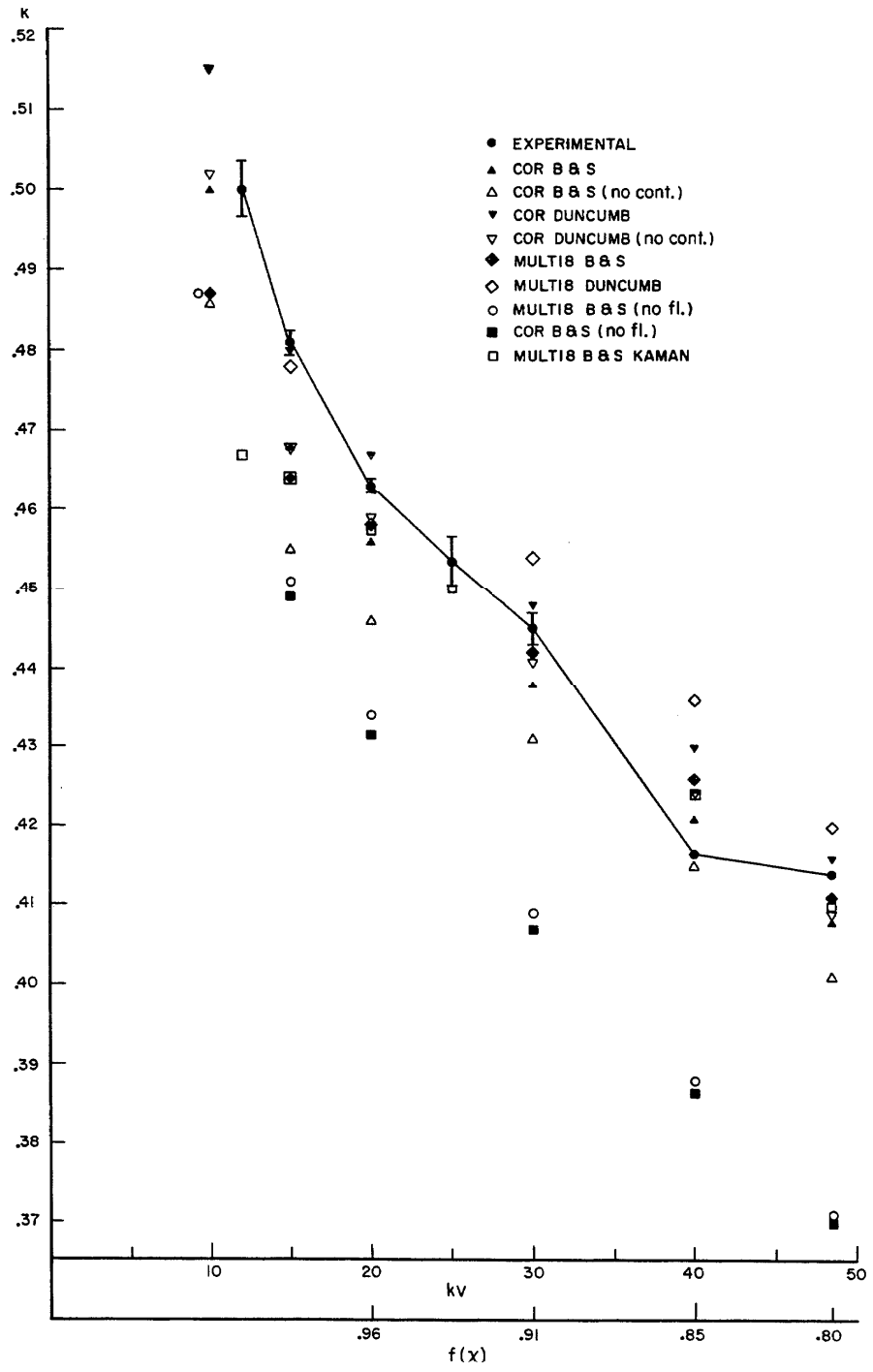

Figure 4. Experimental and theoretical intensity ratios of copper Kα for a nominally Au60-Cu40 alloy.

observed range of k values [19]. To obtain an estimate of the standard deviation of the mean value reported, the estimates, s, should be divided by the square root of the number of data points. Where only one data point was obtained, no value for s is reported.

2. A plot of k/C as a function of k is shown for each SRM set and each measured x-ray line (Figures 5 to 13, Appendix 1). This graph provides an estimator of precision, particularly for single measurements.

3. A table for each SRM set and element compares the experimentally obtained k values with theoretically predicted values for a nominal concentration of 0.4 in the element being investigated (Tables 13 to 16, Appendix 1). Besides the lines measured, operating voltages, experimental k values (k_{ex}), and their estimated standard deviation, s_{ex}, these tables contain: a. the value of k calculated by the computer program COR [20], with use of the values for the mean excitation potential, J, proposed by Berger and Seltzer [21] - this value of k is called k_{COR}; b. the difference $k_{exp} - k_{COR,B-S}$, called Δk_{ex}; c. the absorption function $f(\chi)$ [15], for primary radiation, according to COR; d. the difference in k obtained when the x-ray mass absorption coefficients recently proposed by B. L. Bracewell and W. J. Veigele [22] are substituted for those published earlier by Heinrich [23] and normally used in COR ($\Delta k(\mu/\rho)$) (See Table 17, Appendix 1); e. the difference in k obtained when the J values of Duncumb [16] are substituted for those of Berger and Seltzer ($\Delta k(J)$) (See Table 18, Appendix 1); f. the difference in k obtained when the corrections for fluorescence by the continuum are omitted in COR ($\Delta k(cont)$); and g. the difference in k obtained when the program MULTI 8 [24] is used rather than COR, with the fluorescence due to continuous radiation being disregarded in both programs ($\Delta k(prog)$).

The differences between k_{ex} and k_{COR} give an indication of the accuracy of theoretical correction procedures which are widely used at present. The function $f(\chi)$ and the value of $\Delta k(\mu/\rho)$ indicate how sensitive the value of k is to changes in the mass attenuation coefficients and in the analytical form of the absorption correction. The values of $\Delta k(J)$ are a yardstick for sensitivity of the procedure to variations in the model for stopping power. It is not implied that the two sets of values of the mass attenuation coefficients and of J cover the range including the correct values, nor is any preference between the sets implicit in the information which is presented here.

The next column shows the variation of k caused by omitting the correction for continuous fluorescence. When this difference $\Delta k(cont)$ is small, the corresponding correction is insignificant as a potential source of error. The difference $\Delta k(prog)$ in the last column indicates how well the results of MULTI 8 check with those of COR with the continuum fluorescence correction omitted. The main differences, besides continuum fluorescence, are in the stopping power term, which is numerically integrated in COR as a function of energy, while MULTI 8 uses an approximative procedure developed by H. Yakowitz [25], and in the treatment of fluorescence by characteristic lines. In COR, a rigorous treatment of the characteristic fluorescence is used to separately calculate the effects of each major exciting line. In MULTI 8, instead, the approximative procedure of Reed [26] is followed. Hence, in absence of mistakes in the programs, $\Delta k(prog)$ can be expected to be negligibly small, except in the presence of fluorescence due to characteristic lines, and at very low overvoltages where the effects of electron deceleration are critical.

C. Interpretation of Experimental Data

Standard Reference Materials Set 481

Au $L\alpha_1$: In this system, the effects of absorption are negligible while those of the continuum and of the mean excitation potential are significant (~.005). No characteristic fluorescence is present. Within the experimental scatter - which is fairly large - the k values obtained experimentally check reasonably well with those calculated by COR (B-S).

Au Mα: Experimental data at operating voltages below 30 kV show excessive scatter. The form of the 5 kV curve suggests possible surface contamination on the standard. In spite of these limitations, it is obvious that the experimental values deviate significantly from those obtained by calculation. At low voltages (5-20 kV), the stopping power calculation seems to fail. The discrepancy at high energies is probably due to inaccuracy in the absorption correction; the values obtained from the use of the Kaman mass absorption coefficient tables fit reasonably in this case.

Ag $L\alpha_1$, Ag $L\beta_1$: With the exception of the 5-kV measurements, the k values for Ag $L\alpha_1$, and all values for Ag $L\beta_1$, are highly self-consistent; statistical scatter, where measured, is low.

For both lines, the absorption losses are high and the absorption uncertainty is large, particularly at high voltages, since the lines fall into the region between Au M absorption edges. In particular, Ag $L\beta_1$ is exceedingly close to the edge Au M_{II} (See Table 1). With either set of mass absorption coefficients, the experimental k values are consistently low, particularly at high operating voltages. This suggests an inaccuracy in the absorption correction model.

Standard Reference Material Set 482

Au $L\alpha_1$: Measurements at 15 kV and at 40 kV are of low accuracy. It would be quite difficult to obtain accurate measurements at 15 kV, in view of the high critical excitation potential of the line and the high background level. The measurements in the center of the energy range check well with the calculations by COR (B-S); values derived from the J factor of Duncumb are slightly low.

Au $L\beta_1$: The experimental k values available to date are consistently higher than the calculated values. The reason for this is not clear, particularly since the agreement is fairly good for the Au $L\alpha_1$ values. There is no fluorescence by characteristic lines and the absorption losses are insignificant. The main effects to be considered are fluorescence by the continuum and the atomic number effect (electron deceleration and backscatter).

Au Mα: The experimental k values are quite self-consistent. Comparison with computed values indicates a failure of the stopping power correction, observable by the discrepancies at low voltage. This is not surprising, since there is a strong effect of the choice of expressions for stopping power. At high energies, the absorption losses and, hence, the corresponding uncertainty are high. The experimental values decrease more rapidly than predicted by COR.

Cu Kα: The experimental k values are reasonably precise except for extremely low (12 kV) and very high (40-48.5 kV) energies. They check quite well with the values predicted by COR. However, effects of fluorescence by both Au L lines and by the continuum are significant in this system, and introduce some uncertainty which precludes drawing more precise conclusions with respect to the accuracy of the atomic number corrections.

Cu Lα: Experimental data are quite self-consistent except below 10 kV where, apparently, contamination of the specimens and the pure element caused severe errors. In view of the large absorption losses, the experimental fit to the results obtained from COR is surprisingly good. The values for mass attenuation coefficients were, in this case, obtained by extrapolation of the values used in COR. Fluorescent excitation can be neglected, but the absorption uncertainty is very large.

6. ACKNOWLEDGMENTS

The thoughtful cooperation of T. Rice and J. Frettingham of Cominco American, Inc. and H. Hanson, Jr. of the Bureau of the Mint has greatly aided the completion of this project. Assistance from numerous members of the NBS staff has been received in all phases of this work; we would especially like to acknowledge the help of C. Fiori, M. Giles, K. Loraski, B. Scribner, V. Stewart, D. Vieth, J. Baldwin, R. Durst, C. Gifford, G. Hicho, J. Hust, B. Joiner, M. Meyerson, R. Paulson, R. Powell, and R. Rutter.

7. LIST OF REFERENCES

[1] Castaing, R., Doctoral Thesis, U. Paris, 1951.

[2] Thomas, P. M., At. Energy Res. Estab. (Gt. Brit.) Rept. 4593 (1964).

[3] Heinrich, K. F. J., Adv. in X-ray Analysis 11 (Plenum Press, New York, 1968) p. 40.

[4] Poole, D. M., in NBS Special Publ. 298, 93 (1968).

[5] Thomas, P. M., Brit. J. Appl. Phys. 14, 397 (1963).

[6] Duncumb, P. and Shields, P. K., in The Electron Microprobe, T. D. McKinley, K. F. J. Heinrich, and D. B. Wittry, Eds. (J. Wiley and Sons, Inc., New York, 1966) p. 284.

[7] Belk, J. A., Birmingham C.A.T. Tech. Note, MET/26/1964 (1964).

[8] Ziebold, T. O. and Ogilvie, R. E., Anal. Chem. 35, 621 (1963).

[9] Archard, G. D. and Mulvey, T., X-Ray Optics and X-Ray Microanalysis (Academ. Press, New York, 1962) p. 393.

[10] Theisen, R., Quantitative Electron Microprobe Analysis (Springer-Verlag, New York, 1965).

[11] Yakowitz, H. and Heinrich, K. F. J., Mikrochim. Acta 1968, 182.

[12] Heinrich, K. F. J. and Yakowitz, H., Mikrochim. Acta 1968, 905.

[13] Heinrich, K. F. J. and Yakowitz, H., Mikrochim. Acta 1970, 123.

[14] Heinrich, K. F. J. and Yakowitz, H., Proc. Vth Internat. Congress on X-ray Optics and Microanalysis, Tübingen, 1968, G. Möllenstedt and K. H. Gaukler, Eds. (Springer-Verlag, Berlin, 1969) p. 151.

[15] Heinrich, K. F. J., NBS Tech. Note 521 (1970).

[16] Duncumb, P. and Reed, S. J. B., in NBS Special Publ. 298, 133 (1968).

[17] Goldstein, J. I., Majeske, F. J., and Yakowitz, H., Adv. in X-ray Analysis 10, 217 (1967).

[18] Heinrich, K. F. J., Vieth, D., and Yakowitz, H., Adv. in X-ray Analysis 9, (Plenum Press, New York, 1966) p. 208.

[19] Natrella, M. G., Experimental Statistics, NBS Handbook 91, 2-6 (1963).

[20] Scribner, B. F., ed., NBS Tech. Note 542, 25 (1970).

[21] Berger, M. J. and Seltzer, S. R., "Tables of Energy Losses and Ranges of Electrons and Positrons," Natl. Acad. Sci., Nat. Res. Council Publ. 1133, 205 (1964).

[22] Bracewell, B. L. and Veigele, W. J., "Tables of X-ray Mass Attenuation and Absorption Coefficients for 87 Elements at Selected Wavelengths," Report, Kaman Sciences Corporation, Colorado Springs, Col. (1970).

[23] Heinrich, K. F. J., "X-ray Absorption Uncertainty," in The Electron Microprobe (J. Wiley and Sons, Inc., N. Y., 1966) p. 296.

[24] Available on request from the Spectrochemical Analysis Section, NBS, Washington, D. C. 20234.

[25] This procedure, as yet unpublished, is a fit to the curve shown in Figure 5 of reference [13].

[26] Reed, S. J. B., Brit, J. Appl. Phys. 16, 913 (1965).

[27] Scribner, B. F., ed., NBS Tech. Note 422, 34-35 (1968).

[28] Scribner, B. F., ed., NBS Tech. Note 452, 26-30 (1968).

[29] Yakowitz, H. and Heinrich, K. F. J., Metallography 1, 55 (1968).

APPENDIX 1

RESULTS OF ANALYTICAL MEASUREMENTS

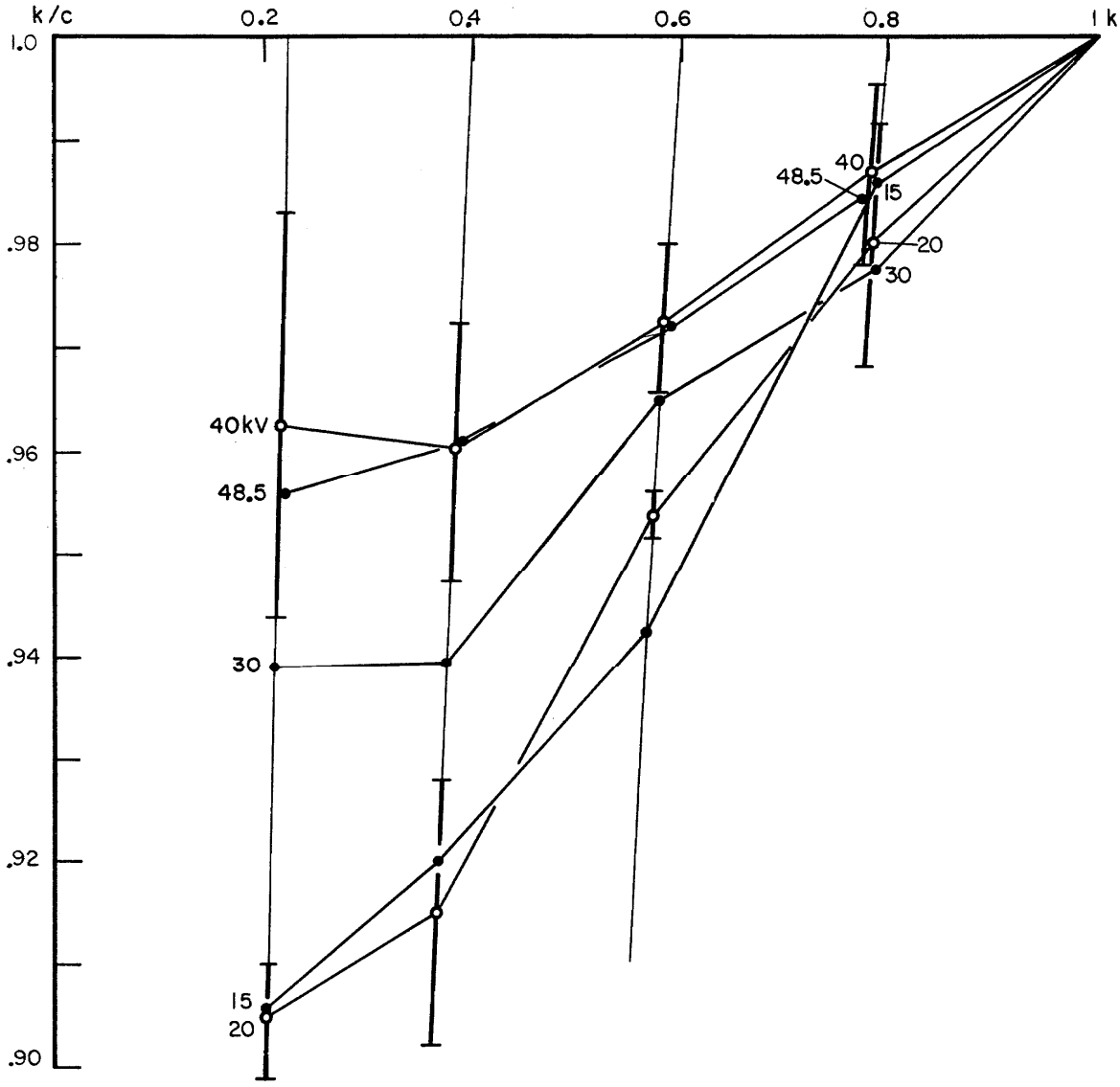

Figure 5. Experimental results on SRM 1181 (Au-Ag) for $AuL\alpha_1$. Bars in Figures 5 through 13 indicate $\pm 1\sigma$ ranges. Points without bars represent single determinations. The numerical values of the data presented in these figures are listed in Tables 9-16.

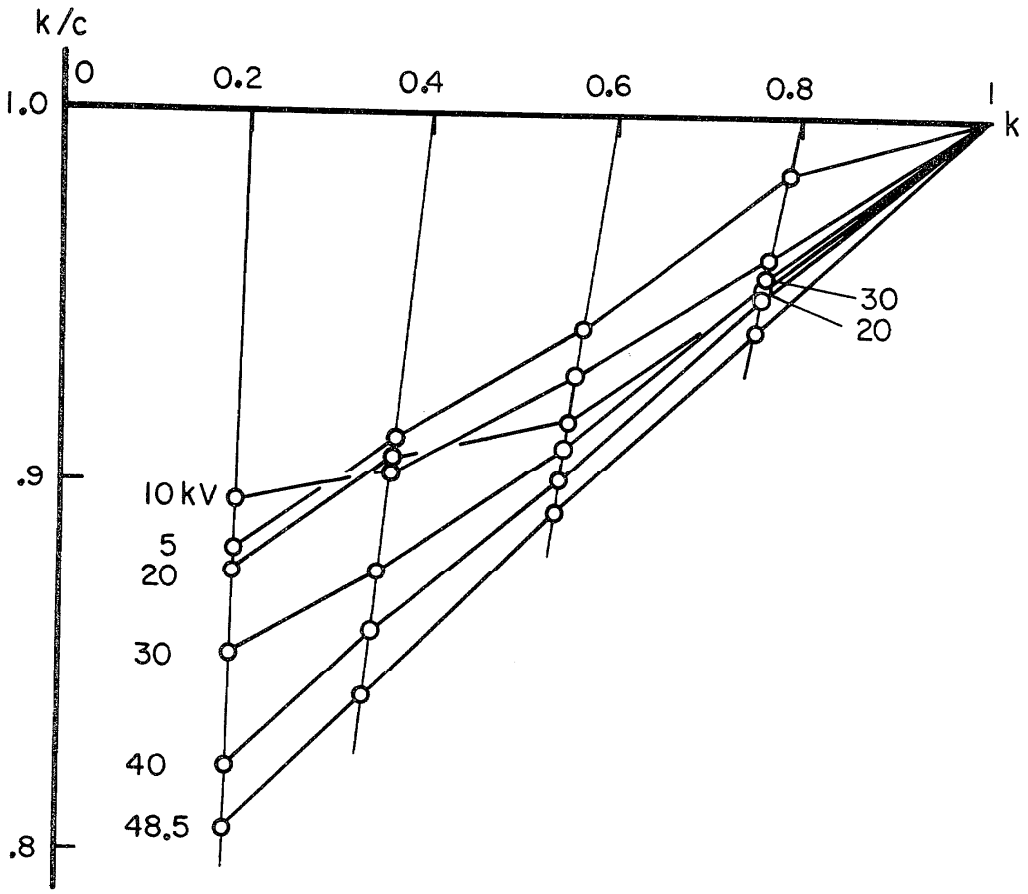

Figure 6. Experimental results on SRM 481 (Au-Ag) for AuMα.

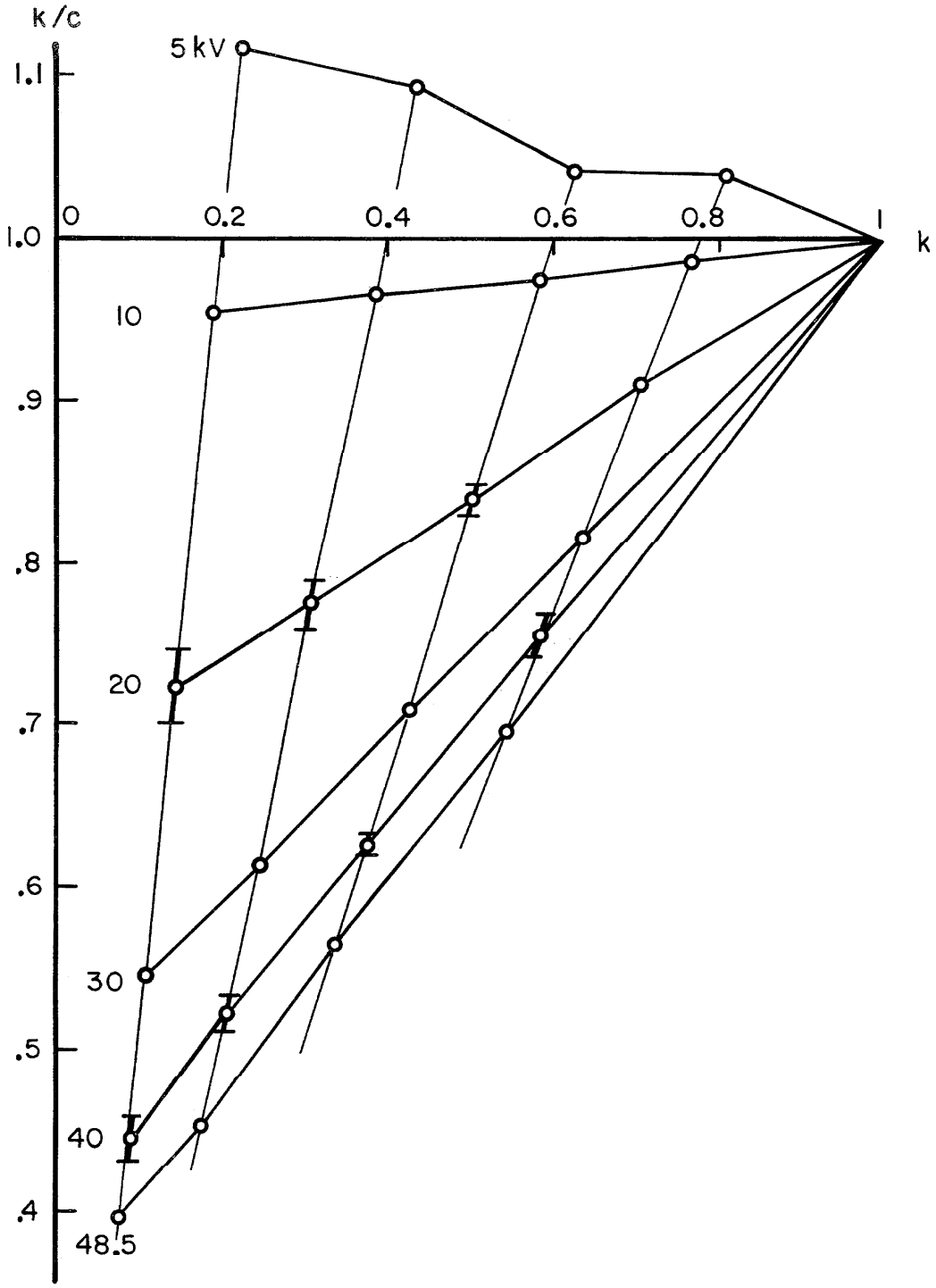

Figure 7. Experimental results on SRM 481 (Au-Ag) for $AgL\alpha_1$.

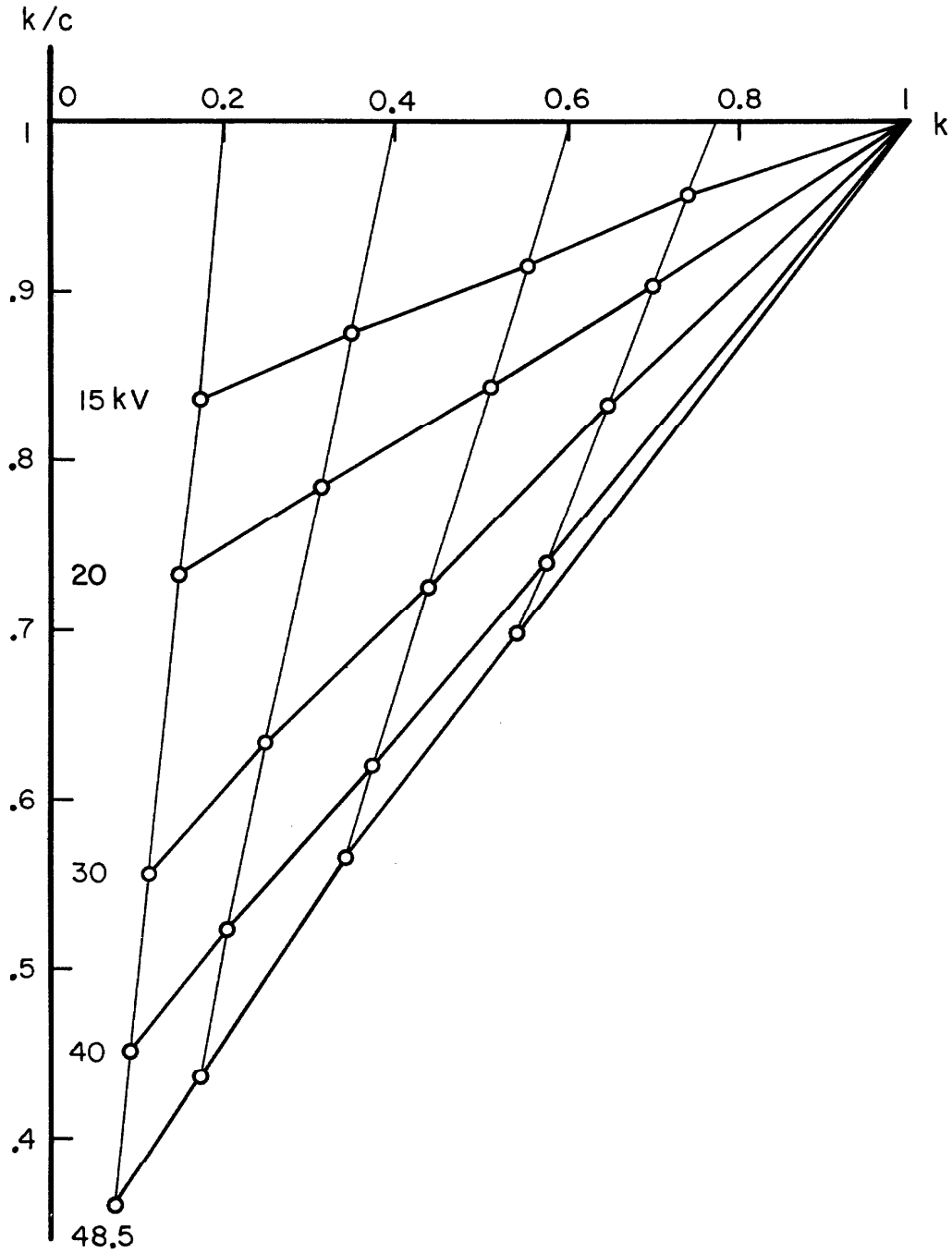

Figure 8. Experimental results on SRM 481 (Au-Ag) for $AgL\beta_1$.

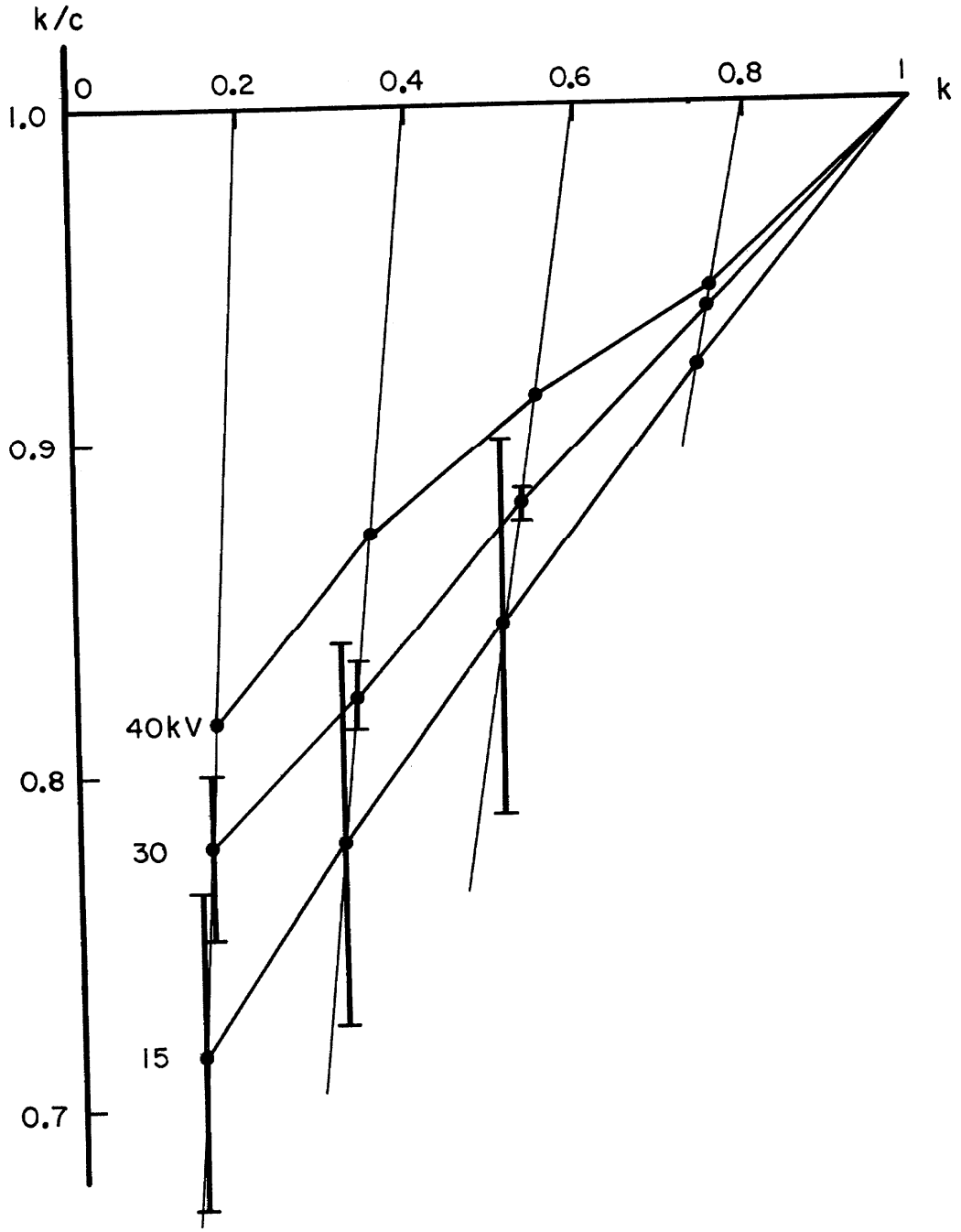

Figure 9a. Experimental results for three voltages on SRM 482 (Au-Cu) for $AuL\alpha_1$.

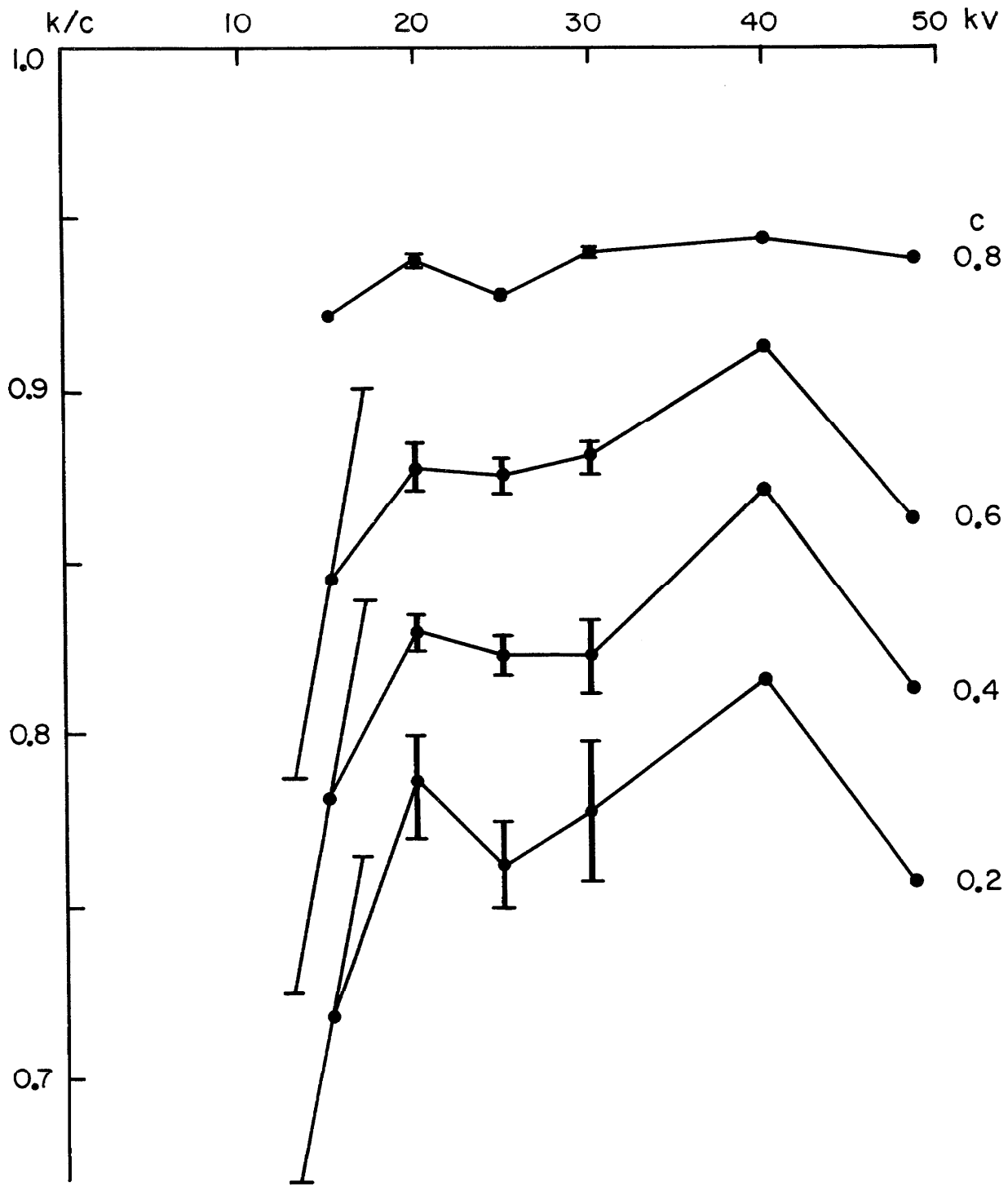

Figure 9b. Experimental results for all the voltages on SRM 482 (Au-Cu) for $AuL\alpha_1$.

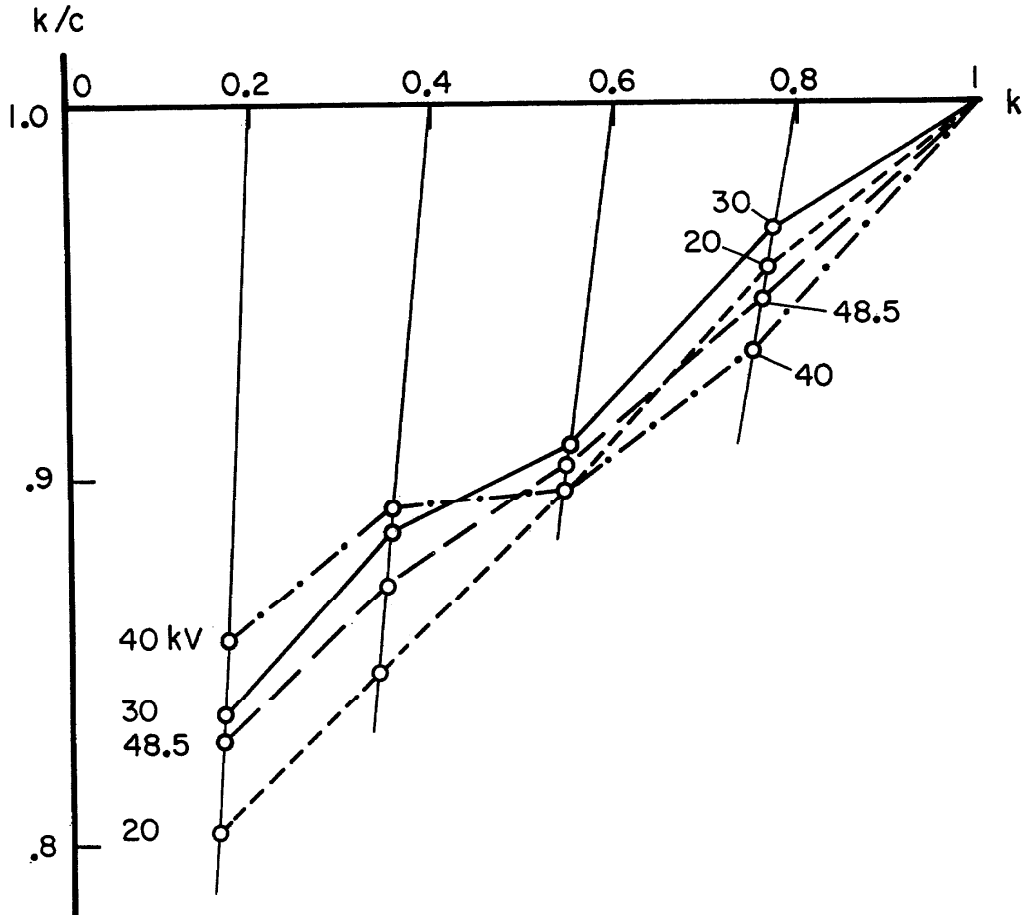

Figure 10. Experimental results on SRM 482 (Au-Cu) for $AuL\beta_1$.

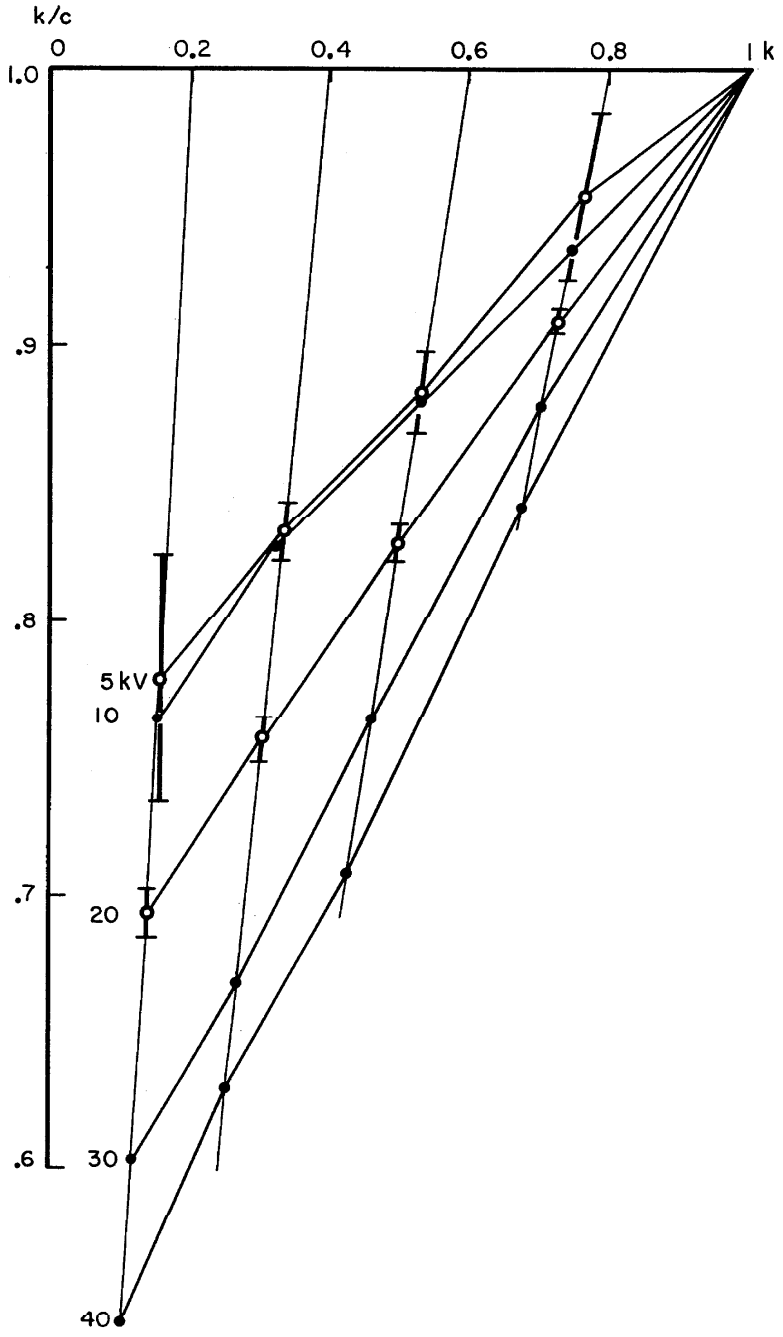

Figure 11. Experimental results on SRM 482 (Au-Cu) for AuMα.

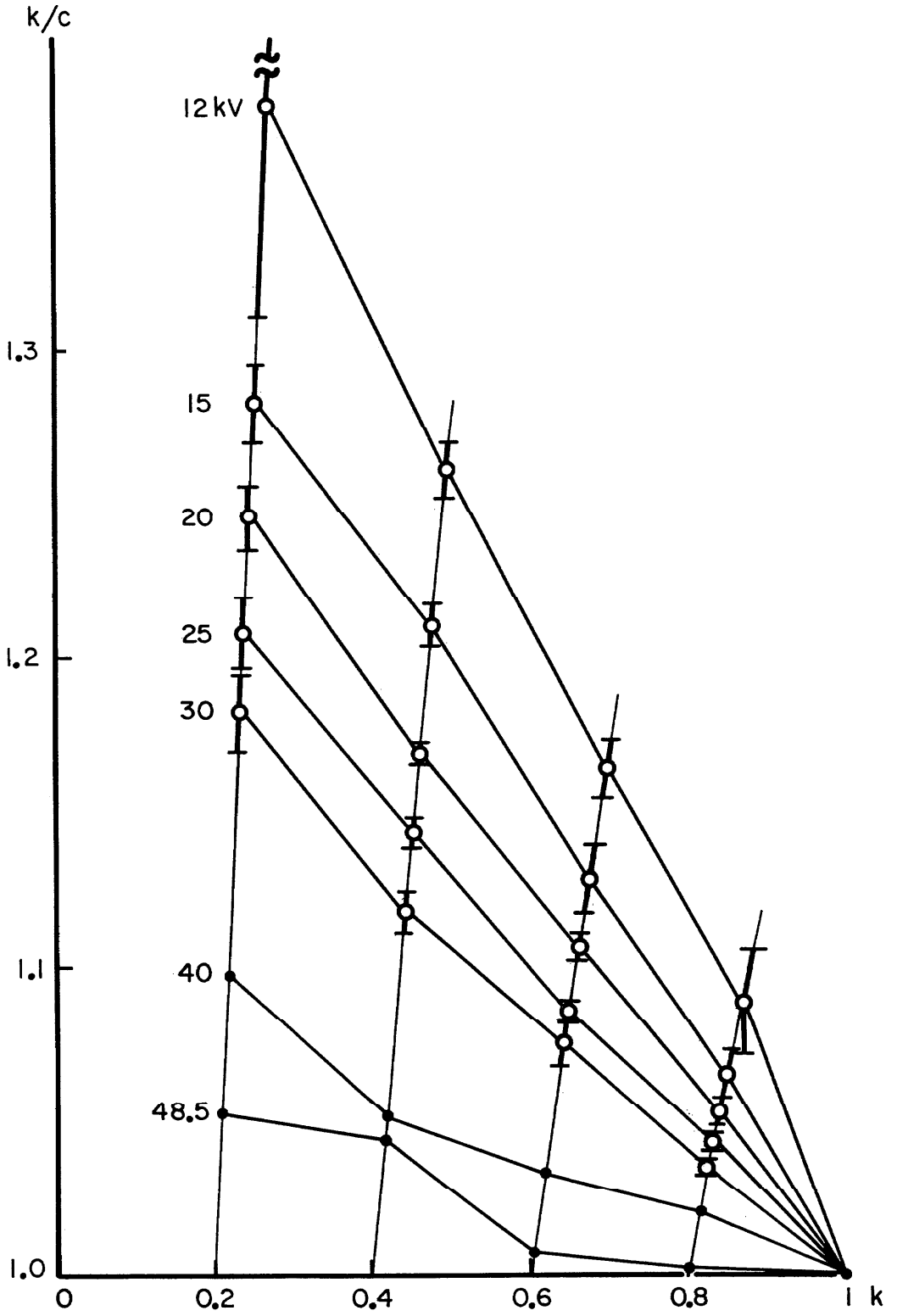

Figure 12. Experimental results on SRM 482 (Au-Cu) for CuKα.

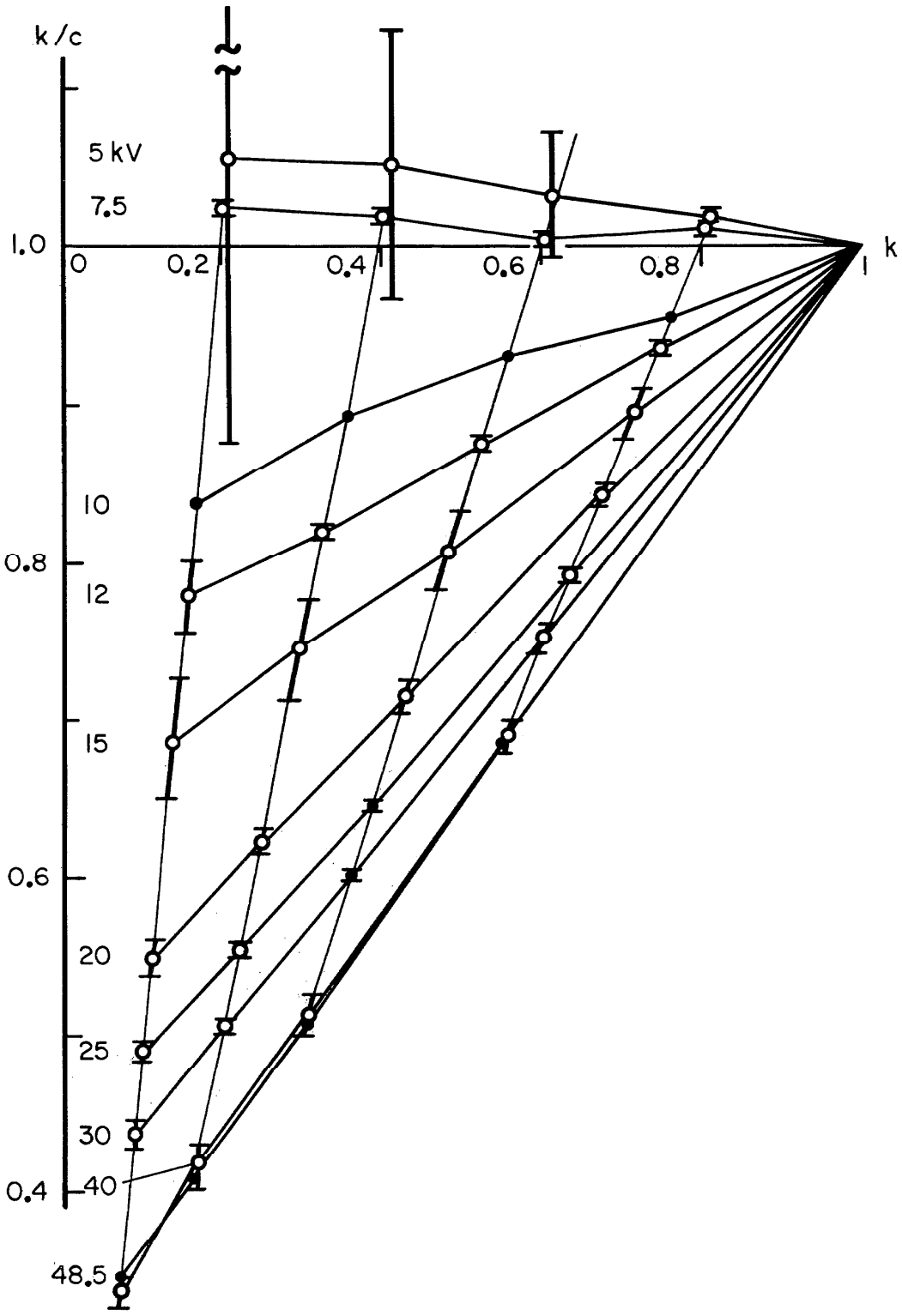

Figure 13. Experimental results on SRM 482 (Au-Cu) for CuLα.

Table 9. Au-Ag, SRM 481 - Results for Au

		C_{Au}:	.2243		.4003		.6005		.8005	
Line	kV	Operators[a]	k	s[b]	k	s	k	s	k	s
$AuL\alpha_1$	15	111	0.203		0.368		0.566		0.789	
	20	122, 311	.203	.001	.366	.005	.573	.001	.783	.010
	30	111	.211		.376		.580		.783	
	40	111, 311	.216	.004	.384	.005	.584	.004	.790	.007
	48.5	111	.214		.385		.584		.788	
$AuM\alpha$	5	111	.198		.365		.566		.789	
	10	111	.201		.362		.559		.771	
	20	111	.197		.364		.551		.764	
	30	111	.192		.351		.547		.766	
	40	111	.185		.344		.541		.761	
	48.5	111	.181		.337		.537		.755	

[a] Operators: First digit identifies the operator, second digit gives the number of sets of measurements (i.e., experiments), third digit indicates the total number of data points obtained by the operator.

[b] s: Estimate of the standard deviation of a single measurement, obtained from the range of measured values [19].

Table 10. Au-Ag, SRM 481 - Results for Ag

			C_{Ag}: .1996		.3992		.5993		.7758	
Line	kV	Operators	k	s	k	s	k	s	k	s
$AgL\alpha_1$	5	111	0.223		0.436		0.624		0.807	
	10	111	.191		.386		.584		.764	
	20	122, 311	.144	.005	.309	.007	.504	.005	.706	.005
	30	111	.109		.245		.426		.636	
	40	111, 311	.0887	.0031	.208	.003	.375	.002	.586	.012
	48.5	111	.0795		.181		.339		.542	
$AgL\beta_1$	15	111	.167		.349		.548		.742	
	20	111	.146		.312		.506		.700	
	30	111	.112		.253		.436		.645	
	40	111	.0898		.209		.368		.574	
	48.5	111	.0720		.175		.340		.542	

See footnotes to Table 9.

Table 11. Au-Cu, SRM 482 - Results for Cu

			C_{Cu}: .1983		.3964		.5992		.7985	
Line	kV	Operators	k	s	k	s	k	s	k	s
CuKα	12	212	0.273	0.014	0.500	0.003	0.698	0.006	0.869	0.013
	15	111, 212	.254	.003	.480	.002	.676	.006	.851	.006
	20	134, 311	.247	.002	.464	.001	.663	.003	.841	.003
	25	225	.240	.002	.453	.002	.651	.002	.834	.001
	30	122, 212	.235	.004	.443	.002	.644	.004	.826	.002
	40	111	.218		.416		.616		.815	
	48.5	111	.209		.414		.604		.800	
$CuL\alpha_1$	5	111, 311	.210	.036	.417	.033	.619	.024	.815	.004
	7.5	212	.203	<.001	.404	<.001	.604	.003	.809	.005
	10	111	.166		.354		.557		.764	
	12	212	.155	.004	.325	.002	.524	.001	.747	.002
	15	111, 212	.136	.008	.295	.013	.484	.015	.716	.013
	20	123	.109	.003	.247	.003	.428	.007	.672	.005
	25	225	.097	.001	.219	.001	.387	.002	.632	.004
	30	122, 212	.087	.002	.200	.002	.360	.002	.602	.004
	40	122	.067	.002	.166	.005	.313	.008	.550	.010
	48.5	111	.069		.161		.304		.544	

See footnotes to Table 9.

Table 12. Au-Cu, SRM 482 - Results for Au

			C_{Au}: .2012		.4010		.6036		.8015	
Line	kV	Operators	k	s	k	s	k	s	k	s
$AuL\alpha_1$	15	111, 212	0.145	0.009	0.313	0.023	0.511	0.032	0.740	0.036
	20	122	.158	.003	.333	.001	.531	.004	.752	.001
	25	225	.154	.003	.331	.002	.529	.003	.745	.002
	30	111, 223	.157	.004	.331	.004	.533	.005	.754	.005
	40	111	.164		.350		.552		.758	
	48.5	111	.152		.326		.521		.751	
$AuL\beta_1$	20	111	.162		.341		.542		.766	
	30	111	.168		.355		.549		.775	
	40	111	.172		.358		.541		.749	
	48.5	111	.167		.350		.545		.760	
$AuM\alpha$	5	111, 311	.157	.009	.334	.004	.533	.009	.765	.024
	10	111	.154		.332		.531		.749	
	20	123, 311	.140	.002	.304	.003	.500	.004	.728	.003
	30	111	.122		.275		.462		.704	
	40	111	.110		.253		.428		.675	

See footnotes to Table 9.

Table 13. Au-Ag, SRM 481 - Test calculations for Au

$C_{Au} = .4003$

Line	kV	k_{ex}	s_{ex}	k_{COR}	Δk_{ex}	$f(\chi)$	Δk (μ/ρ)	Δk (J)	Δk (cont)	Δk (prog)
$AuL\alpha_1$	15	0.368		0.360	+0.008	0.99	$\pm$0.000	-0.005	-0.003	$\pm$0.000
	20	.366	.005	.369	- .003	.97	$\mp$ .001	- .005	- .003	$\mp$ .002
	30	.376		.376	$\pm$ .000	.92	+ .001	- .005	- .004	- .001
	40	.384	.005	.379	$\mp$ .005	.87	+ .001	- .004	- .004	$\pm$ .000
	48.5	.385		.380	+ .005	.83	- .002	- .004	- .003	$\mp$ .001
$AuM\alpha$	5	.365		.343	+ .022	.96		- .014	$\pm$ .000	- .005
	10	.362		.357	+ .005	.87	- .002	- .010	$\mp$ .001	- .002
	20	.364		.360	+ .004	.67	- .006	- .007	$\pm$ .000	- .001
	30	.351		.358	- .007	.50	- .011	- .006	$\mp$ .001	+ .002
	40	.344		.355	- .011	.38	- .014	- .005	- .001	+ .002
	48.5	.337		.352	- .015	.30	- .017	- .005	- .001	+ .003

Table 14. Au-Ag, SRM 481 - Test calculations for Ag

$C_{Ag} = .3992$

Line	kV	k_{ex}	s_{ex}	k_{COR}	Δk_{ex}	f(χ)	Δk (μ|ρ)	Δk (J)	Δk (cont)	Δk (prog)
$AgL\alpha_1$	5	0.436		0.449	-0.013	0.97	-0.001	+0.012	±0.000	+0.003
	10	.386		.402	- .016	.87	- .004	+ .007	± .000	+ .002
	20	.309	.007	.333	- .024	.64	- .009	+ .005	± .000	± .000
	30	.245		.283	- .038	.46	- .011	+ .004	± .000	- .001
	40	.208	.003	.249	- .041	.34	- .011	+ .002	- .002	- .001
	48.5	.181		.227	- .046	.27	- .011	+ .003	- .002	- .001
$AgL\beta_1$	15	.349		.358	- .009	.75	± .000	+ .006	± .000	+ .002
	20	.312		.323	- .011	.64	± .001	+ .005	± .000	+ .001
	30	.253		.269	- .016	.46	+ .001	+ .003	- .001	+ .001
	40	.209		.232	- .023	.34	+ .002	+ .002	- .002	+ .001
	48.5	.175		.209	- .034	.26	+ .001	+ .002	- .002	+ .001

Table 15. Au-Cu, SRM 482 - Test calculations for Au

C_{Au} = .4010

Line	kV	k_{ex}	s_{ex}	k_{COR}	Δk_{ex}	f(χ)	Δk (μ|ρ)	Δk (J)	Δk (cont)	Δk (prog)
AuLα$_1$	15	0.313	0.023	0.321	-0.008	0.98	±0.000	-0.011	+0.005	-0.001
	20	.333	.001	.332	+ .001	.95	∓ .000	- .010	+ .006	- .002
	25	.331	.002	.336		.92				
	30	.331	.004	.336	- .005	.89	± .000	- .010	+ .006	- .002
	40	.350		.332	+ .018	.82	∓ .002	- .009	+ .006	- .002
	48.5	.326		.327	- .001	.75	+ .001	- .008	+ .005	- .001
AuLβ$_1$	20	.341		.332	+ .009	.98	± .000	- .010	+ .004	- .001
	30	.355		.340	+ .015	.93	∓ .000	- .010	+ .006	- .002
	40	.358		.339	+ .019	.88	∓ .000	- .009	+ .007	- .002
	48.5	.350		.336	+ .014	.83	∓ .000	- .008	+ .008	- .002
AuMα	5	.334	.004	.304	+ .030	.95	± .000	- .026	± .000	- .006
	10	.332		.315	+ .017	.83	∓ .002	- .019	∓ .000	- .002
	20	.304	.003	.300	+ .004	.59	- .005	- .013	∓ .001	+ .001
	30	.275		.282	- .007	.41	- .008	- .017	+ .001	+ .002
	40	.253		.265	- .012	.29	- .010	- .009	± .000	+ .003

Table 16. Au-Cu, SRM 482 - Test calculations for Cu

$C_{Cu} = .3964$

Line	kV	k_{ex}	s_{ex}	k_{COR} (B-S)	Δk_{ex}	f(χ)	Δk (μ|ρ)	Δk (J)	Δk (cont)	Δk (prog)
CuKα	12	0.500	0.003			0.99	±0.000			
	15	.480	.002	.468	+ .012	.98	± .000	+ .012	- .013	+ .009
	20	.461	.001	.456	+ .005	.96	± .000	+ .011	- .010	+ .012
	25	.453	.002	.447		.93				
	30	.443	.002	.438	+ .005	.91	- .001	+ .010	- .007	+ .011
	40	.416		.421	- .005	.85	- .002	+ .009	- .006	+ .011
	48.5	.414		.408	+ .006	.80	- .001	+ .008	- .007	+ .010
$CuL\alpha_1$	5	.417	.033	.439	- .022	.82	- .012	+ .032	± .000	± .000
	7.5	.404	<.001	.389		.71				
	10	.354		.350	+ .004	.59	- .023	+ .016	± .000	- .004
	12	.325	.002	.325		.52				
	15	.295	.013	.295	± .000	.42	- .029	+ .012	- .001	- .004
	20	.247	.003	.258	- .011	.30	- .031	+ .010	± .000	- .005
	25	.219	.001	.233		.22				
	30	.200	.002	.215	- .015	.17	- .034	+ .007	- .001	- .004
	40	.166	.005	.191	- .025	.10	- .035	+ .005	- .002	- .003
	48.5	.161		.177	- .016	.07	- .036	+ .005	- .001	- .003

Table 17. Mass absorption coefficients used in the preparation of Tables 13 to 16

	Cu		Au	
Sources:	[23]	[22]	[23]	[22]
Line				
CuKα	53.5	52.8	208	210
CuLα	2079*	1907	7030*	8181
AuMα	2034	2025	1124	1016
$AuL\alpha_1$	246	245	128	132
$AuL\beta_1$	158	162	83.4	89.2

*Values obtained by extrapolation

	Ag		Au	
Sources:	[23]	[22]	[23]	[22]
Line				
$AgL\alpha_1$	522	540	1961	2155
$AgL\beta_1$	466	477	2052	2059
AuMα	1266	1277	1124	1016
$AuL\alpha_1$	130	130	128	132

Table 18. Mean excitation potentials

	Element		
	Cu	Ag	Au
Source			
[21]	314	487	797
[16]	377	637	1071

APPENDIX 2

CERTIFICATES OF ANALYSIS FOR SRM'S 481 AND 482

U. S. Department of Commerce
Maurice H. Stans
Secretary

National Bureau of Standards
A. V. Astin, Director

Certificate of Analysis

Standard Reference Material 481
Gold-Silver Wires for Microprobe Analysis

These standard reference materials are designed for use in quantitative elemental microprobe analysis. Although the selection of this particular system was circumscribed by the requirements of standard reference materials for electron probe microanalysis, the materials will be equally useful for other micro techniques. Accurate chemical characterization and the achievement of homogeneity on a microscopic scale was given special emphasis.

SRM 481 wire	Color code	Nominal comp	Cominco American[a]	U.S. Bureau of the Mint[b]		NBS[c]		Average Value[d]	
			Au	Au	Ag	Au	Ag	Au	Ag
			Percent by weight						
A	Gold	Au100	---	---	---	---	---	100.0_0	---
B	Gray	Au80–Ag20	80.00	80.02	20.00	80.13	19.93	80.0_5	19.9_6
C	Yellow	Au60–Ag40	60.01	60.11	39.85	60.04	39.98	60.0_5	39.9_2
D	Blue	Au40–Ag60	39.99	40.03	59.90	40.06	59.96	40.0_3	59.9_3
E	Red	Au20–Ag80	22.42	22.42	77.59	22.46	77.56	22.4_3	77.5_8
F	Silver	Ag100	---	---	---	---	---	---	100.0_0

[a] The fire assay method was employed for the determination of Au by Cominco American.

[b] At the U.S. Bureau of the Mint, Au was determined by fire assay and Ag was determined by titration as AgCl.

[c] At NBS, Au was determined from the residue after treatment of the alloys with HNO_3. The Au residue was dissolved in aqua regia, filtered, the Au precipitated by sulfurous acid, and weighed. Ag was determined gravimetrically as AgCl in all four alloys, and also coulometrically in the 80 percent Ag alloy.

[d] The results of individual laboratories agree within a range of ± 0.1 percent absolute from the average values. The agreement between results by the different methods and analysts, and the summation of results close to 100 percent for each binary alloy, indicate that the averages are free from significant bias.

The set of standard reference materials, SRM 481, consists of six wires each having a diameter of approximately 0.5 mm and a length of approximately 5 cm. For identification, the four alloy wires were covered with an easily removable colored coating.

The overall direction and coordination of technical measurements leading to certification were performed under the chairmanship of B. F. Scribner.

The technical and support aspects involved in the preparation, certification, and issuance of these standards were coordinated through the Office of Standard Reference Materials by R. E. Michaelis.

Washington, D. C. 20234
February 14, 1969

(over)

W. Wayne Meinke, Chief
Office of Standard Reference Materials

PREPARATION AND PURITY: The standards were prepared by Cominco American Inc. in the form of wires approximately 150 meters long. The end members of the series, as well as the starting materials for the alloys, were of the highest purity grade and precautions were taken to minimize contamination. Two of the alloy standards were heat-treated at NBS to improve microhomogeneity. The pure metal standards were examined by the residual resistivity ratio technique and the total of electrically active impurities in each was estimated to be about 0.001 percent. The gold-silver wires were examined spectrographically for metallic impurities; no significant impurities were found at detection limits ranging from 0.0001 to 0.010 percent.

LONGITUDINAL HOMOGENEITY: Variation in composition along the full length of each alloy wire was investigated by electron probe microanalysis for areas 25 μm diameter on cross sections at three to five positions along the wire including the two ends. The observed differences in composition for the positions, expressed as the range between the highest and lowest values for each alloy, were as follows:

Nominal Composition	Au80	Au60	Au40	Au20
Observed range[a]	0.3%	0.6%	0.3%	0.5%

Homogeneity along the wires was also tested by measurement of the residual resistivity ratio. These measurements indicated that the variation (macroscopic) of composition along all standard wires was less than 0.1 percent absolute. Further information on longitudinal homogeneity of the wires was obtained by determinations of Au at the extreme ends of the alloy wires by the Bureau of the Mint; the data also indicate that the extreme variation along the wires is less than 0.1 percent absolute.

TRANSVERSE AND MICRO HOMOGENEITY: Variation in composition within the above mentioned cross sections of the wires was investigated by electron probe microanalysis. For each cross section, measurements were made along two diagonals at right angles. On each diagonal, determinations were made at 25 points, 1 μm or less in diameter, starting and ending at approximately 25 μm from the edge. For each alloy, the element which could be determined with the better precision was used in the evaluation. The variation was calculated in terms of the standard deviation for an individual determination for each traverse. In the table below, the variation is presented as the range between the lowest and highest observed standard deviations for the six to eight traverses performed on each alloy.

Nominal Composition	Element Determined	Range of Standard Deviation for Traverses[a]
Au80	Ag	0.08 – 0.11%
Au60	Au	.08 – .16
Au40	Au	.08 – .13
Au20	Au	.12 – .37

The homogeneity on a microscopic scale was further investigated by performing quantitative measurements in two arrays of 10 × 10 points (1 μm diameter) on each of the cross sections. The distance between adjacent points was 3.5 μm. This was repeated on several cross sections so that 6 to 8 arrays were obtained on each alloy. For the element which could be measured with better precision, the range is given between the lowest and highest observed standard deviation for an individual determination for the 6 to 8 arrays for each alloy.

Nominal Composition	Element Evaluated	Range of Standard Deviations for Arrays[a]
Au80	Ag	0.09 – 0.15 %
Au60	Au	.18 – .57
Au40	Au	.19 – .25 ,
Au20	Au	.11 – .66

(Note: This range and the two ranges in the following tables are close to the precision of the method and should be considered upper limits of estimates of inhomogeneity.)

Extensive homogeneity studies were performed with the electron probe microanalyzer at NBS by M. A. Giles, R. L. Myklebust, C. E. Fiori, and K. F. J. Heinrich. Measurements of residual resistivity ratio were made at NBS, Boulder, Colorado, by R. L. Rutter, J. G. Hust, and R. L. Powell. Heat treatment of the alloys at NBS was performed by G. E. Hicho and M. R. Meyerson. Spectrographic survey analyses were made at NBS by V. C. Stewart. Determinations of composition were made at Cominco American, Inc., Spokane, Washington, by T. A. Rice; at the U.S. Bureau of the Mint, Washington, D. C., by H. G. Hanson, Jr.; and at NBS by R. A. Durst, G. Marinenko, and C. E. Champion.

U. S. Department of Commerce
Maurice H. Stans
Secretary

National Bureau of Standards
A. V. Astin, Director

Certificate of Analysis

STANDARD REFERENCE MATERIAL 482
Gold-Copper Wires for Microprobe Analysis

These standard reference materials are designed for use in quantitative elemental microprobe analysis. Although the selection of this particular system was circumscribed by the requirements of standard reference materials for electron probe microanalysis, the materials will be equally useful for other micro techniques. Accurate chemical characterization and the achievement of homogeneity on a microscopic scale were given special emphasis.

SRM 482 wire	Color code	Nominal composition	Cominco American[a]	U.S. Bureau of the Mint[b]		NBS[c]		Average value[d]	
			Au	Au	Cu	Au	Cu	Au	Cu
			Percent by weight						
A	Gold	Au100	–	–	–	–	–	100.0_0	–
B	Gray	Au80 – Cu20	80.10	80.13	19.81	80.21	19.85	80.1_5	19.8_3
C	Blue	Au60 – Cu40	60.30	60.37	39.66	60.41	39.62	60.3_6	39.6_4
D	Yellow	Au40 – Cu60	40.12	40.06	59.88	40.11	59.97	40.1_0	59.9_2
E	Red	Au20 – Cu80	20.04	20.12	79.84	20.21	79.86	20.1_2	79.8_5
F	Copper	Cu100	–	–	–	–	–	–	100.0_0

[a] The fire assay method was employed for the determination of Au by Cominco American.

[b] At the U. S. Bureau of the Mint, Au was determined by fire assay and Cu was determined by electrodeposition.

[c] At NBS, Au was determined by precipitation from solution; Cu was determined by electrodeposition.

[d] The results of individual laboratories agree within a range of ± 0.1% absolute from the average values. The agreement between results by the different methods and analysts, and the summation of results close to 100% for each binary alloy, indicate that the averages are free from significant bias.

The set of standard reference materials, SRM 482, consists of six wires each having a diameter of approximately 0.5 mm and a length of approximately 5 cm. For identification, the four alloy wires were covered with an easily removable colored coating.

The overall direction and coordination of technical measurements leading to certification were performed under the chairmanship of B. F. Scribner.

The technical and support aspects involved in the preparation, certification, and issuance of these standards were coordinated through the Office of Standard Reference Materials by R. E. Michaelis.

Washington, D. C. 20234
June 6, 1969

W. Wayne Meinke, Chief
Office of Standard Reference Materials

(over)

PREPARATION AND PURITY: The standards were prepared by Cominco American, Inc. in the form of wires approximately 150 meters long. The end members of the series, as well as the starting materials for the alloys, were of the highest purity grade and precautions were taken to minimize contamination. Two of the alloy standards were heat-treated at NBS to improve microhomogeneity. The pure metal standards were examined by the residual resistivity ratio technique and the total of electrically active impurities in each was estimated to be about 0.001%. The gold-copper wires were examined spectrographically for metallic impurities; no significant impurities were found at detection limits ranging from 0.0001 to 0.010%.

LONGITUDINAL HOMOGENEITY: Variation in composition along the full length of each alloy wire was investigated by electron probe microanalysis for areas 25 μm diameter on cross sections at three positions along the wire including the two ends. The observed differences in composition for the positions, expressed as the range between the highest and lowest values for each alloy, were as follows:

Nominal Composition	Au80	Au60	Au40	Au20
Observed range*	0.3%	0.7%	0.9%	0.9%

Homogeneity along the wires was also tested by measurement of the residual resistivity ratio. These measurements indicated that the variation (macroscopic) of composition along all standard wires was less than 0.1% absolute. Further information on longitudinal homogeneity of the wires was obtained by determinations of Au at the extreme ends of the alloy wires by the Bureau of the Mint; the data also indicate that the extreme variation along the wires is less than 0.1% absolute.

TRANSVERSE AND MICRO HOMOGENEITY: Variation in composition within the above mentioned cross sections of the wires was investigated by electron probe microanalysis. For each cross section, measurements were made along two diagonals at right angles. On each diagonal, determinations were made at 25 points, 1 μm or less in diameter, starting and ending at approximately 25 μm from the edge. For each alloy, the element which could be determined with the better precision was used in the evaluation. The variation was calculated in terms of the standard deviation for an individual determination for each traverse. In the table below, the variation is presented as the range between the lowest and highest observed standard deviations for the six traverses performed on each alloy.

Nominal Composition	Element Determined	Range of Standard Deviations for Traverses*
Au80	Cu	0.09 – 0.24%
Au60	Cu	.16 – .27
Au40	Au	.13 – .23
Au20	Au	.13 – .20

The homogeneity on a microscopic scale was further investigated by performing quantitative measurements in two arrays of 10 × 10 points (1 μm diameter) on each of the cross sections. The distance between adjacent points was 3.5 μm. This was repeated on several cross sections so that 6 arrays were obtained on each alloy. For the element which could be measured with better precision, the range is given between the lowest and highest observed standard deviation for an individual determination for the 6 arrays for each alloy.

Nominal Composition	Element Determined	Range of Standard Deviations for Arrays*
Au80	Cu	0.19 – 0.28%
Au60	Cu	.28 – .37
Au40	Au	.25 – .31
Au20	Au	.12 – .20

*The ranges indicated are close to the precision of the method and should be considered upper limits of estimates of inhomogeneity.

Extensive homogeneity studies were performed with the electron probe microanalyzer at NBS by M. A. Giles, D L. Vieth, R. L. Myklebust, C. E. Fiori, and K. F. J. Heinrich. Measurements of residual resistivity ratio were made at NBS, Boulder, Colorado, by R. L. Rutter and R. L. Powell. Heat treatment of the alloys at NBS was performed by G. E. Hicho and M. R. Meyerson. Spectrographic survey analyses were made at NBS by V. C. Stewart. Determinations of composition were made at Cominco American, Inc., Spokane, Washington, by T. A. Rice; at the U. S. Bureau of the Mint, Washington, D. C., by H. G. Hanson, Jr.; and at NBS by J. R. Baldwin and R. A. Durst.

APPENDIX 3
PRELIMINARY HOMOGENEITY TESTING

The preparation, homogenization, and preliminary homogeneity testing of the Au-Ag and Au-Cu alloys extended over a period of more than two years. This Appendix summarizes the preliminary analyses performed during preparation of the alloys. Important points have been extracted from the many reports written during this period and are presented in chronological order.

Final characterization of composition and homogeneity is discussed in Sections Three and Four, respectively.

Dec. 23, 1966 (Au-Ag) The following materials and assay reports were received from Cominco American, Inc.

	Ca	Cr	Fe	Mg	Si	Ag	Al	Pb	Ni
6-9's Cu	0.1*	0.1	1.0	0.2	1.0	2.0	--	--	--
6-9's Ag	0.3	1.0	0.5	0.2	1.0	--	0.1	0.5	--
6-9's Au	0.3	1.0	0.7	0.3	0.7	0.1	--	--	0.3

*All values are in ppm

Alloys	Mass fraction Au
Au20-Ag80	0.1999
Au60-Ag40	0.6001
Au80-Ag20	0.8000
Au40-Ag60	0.3999

Note: No significant differences in the impurity levels between the alloys and the pure elements were observed.

April 25, 1967 The following materials and assay reports were received from Cominco American, Inc.

Alloys	Mass fraction Au
Au60-Cu40	0.603
Au80-Cu20	0.801
Au20-Cu80	0.199
Au40-Cu60	0.401

Note: No significant differences in the impurity levels between the alloys and the pure elements were observed.

June 7, 1967 (Au-Ag) An NBS report on the homogeneity of the Au20-Ag80 alloy concluded that this alloy was unacceptable due to a gold-enriched layer 30 μm thick at the surface of the wire.

Oct. 19, 1967 (Au-Ag) An NBS report on the homogeneity of the Au20-Ag80 alloy found this alloy to be macroscopically homogeneous along the length of the wire. It was, however, microscopically inhomogeneous across the cross-section and therefore unusable.

Oct. 25, 1967 (Au-Ag) An NBS report on the homogeneity of the Au80-Ag20 alloy found this wire to be homogeneous to within 0.005 both along the wire and across the cross-section, except for a very thin region near the edge.

Oct. 27, 1967 (Au-Ag) The Au20-Ag80 wires were submitted to a homogenization heat treatment at NBS.

Nov. 8, 1967 (Au-Ag) An NBS report on the homogeneity of the Au40-Ag60 alloy found this wire to be homogeneous to within 0.005 along the length but inhomogeneous across the cross-section.

(This material was later given the same homogenization heat treatment as the Au20-Ag80.)

Nov. 28, 1967 (Au-Ag) Electronic characterization (residual resistivity ratio) was performed at NBS on two of the alloys. The Au80-Ag20 was homogeneous to within 0.002 and the Au60-Ag40 was ten times worse (0.02).

Feb. 29, 1968 (Au-Cu) Electronic characterization was performed on the Au-Cu alloys at NBS with the following results.

Alloy	Homogeneity Range
Au80-Cu20	0.002
Au60-Cu40	0.0015
Au20-Cu80	0.002
Au40-Cu60	not done - wire too brittle

March 4, 1968 (Au-Ag) Cominco American, Inc. replaced the Au20-Ag80 alloy.

March 14, 1968 Electronic characterization of the pure Au, Ag, and Cu was performed at NBS. Total impurities in each metal are about 10 ppm.

May 24, 1968 (Au-Ag) Electronic characterization of the new Au20-Ag80 alloy at NBS concluded that it was homogeneous to within 0.002.

July 3, 1968 (Au-Cu) A chemical analysis at NBS was performed on the Au40-Cu60 alloy after a homogenization heat treatment. The mass fractions of Au in two samples were 0.4017 and 0.4013; therefore, no Cu was lost.

Aug. 16, 1968 (Au-Cu) A chemical analysis was performed at NBS on the Au20-Cu80 alloy both before and after a homogenization heat treatment.

Au before treatment - 0.2021
Au after treatment - 0.2022

Dec. 16, 1968 (Au-Cu) and (Au-Ag) Electronic characterizations were performed at NBS on the following alloys.

Alloy	Homogeneity Range
Au40-Cu60	0.001
Au40-Ag60	0.002
Au20-Ag80	0.002

Feb. 6, 1969 (Au-Ag) Cominco American, Inc. assayed the new Au20-Ag80 alloy as 0.2242 Au.

April 22, 1969 (Au-Cu) An optical spectrographic analysis at NBS of the Au-Cu alloys found the following impurities in each.

Ag <0.00001, Mg <0.00001, Pb <0.00001, and Si <0.0001.

APPENDIX 4

AUTOMATED TECHNIQUES FOR HOMOGENEITY ANALYSIS

In the preparation of any standard reference material, characterization of composition uniformity is essential. This is to insure that each standard is, within specified limits, the same as any other standard of the same type. In addition, characterization of homogeneity on a microscopic scale is required in the case of standards for microprobe and other micro-analytical techniques. After consultation with other microprobe analysts, we set a goal of producing standards in which the range of concentrations, on either a macro- or micro-scale, do not exceed 0.01. The quantity of data necessary to establish the micro-homogeneity of the two sets of standards described in this report was large (more than 36,000 determinations) and prompted development of the automated data acquisition system and computer program described in this section.

A. Instrumental

An automated data acquisition system [27, 28], referred to as a matrix scanner, has been developed to direct the electron probe beam to different locations on a specimen and to record quantitative analytical data associated with each location. The matrix scanner can be preset to examine test locations arranged in either a straight line or in a two-dimensional grid (raster). The latter arrangement conserves the digital quantitative nature of the information obtained in single-point analysis while providing topographic coverage analogous to continuous area scanning of low resolution.

A schematic block diagram of the matrix scanner is given in Figure 14, and the front panels of the electronic modules are shown in Figure 15. Before examining the details of operation for individual electron modules, it is helpful to

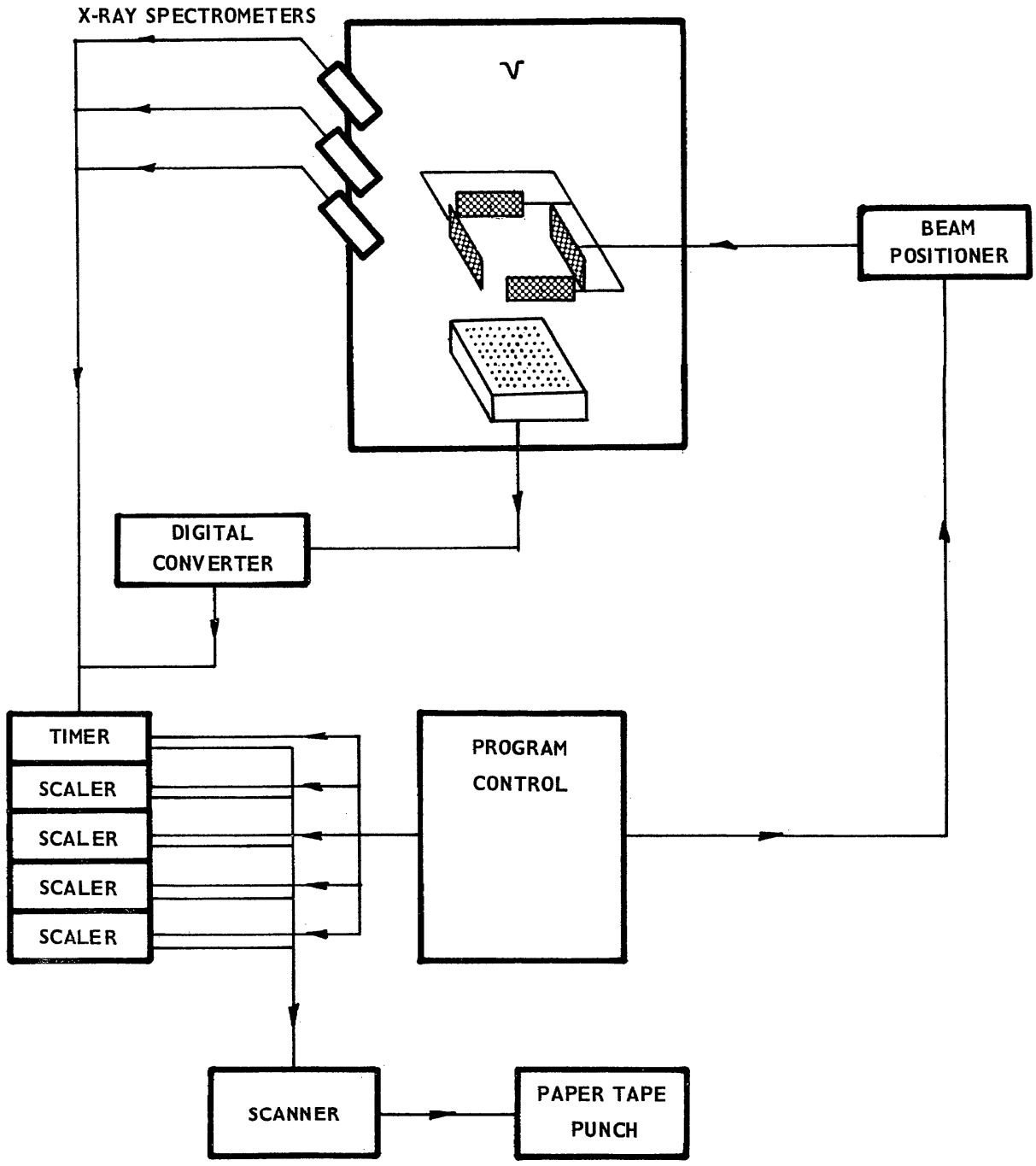

Figure 14. Block diagram of the matrix scanner.

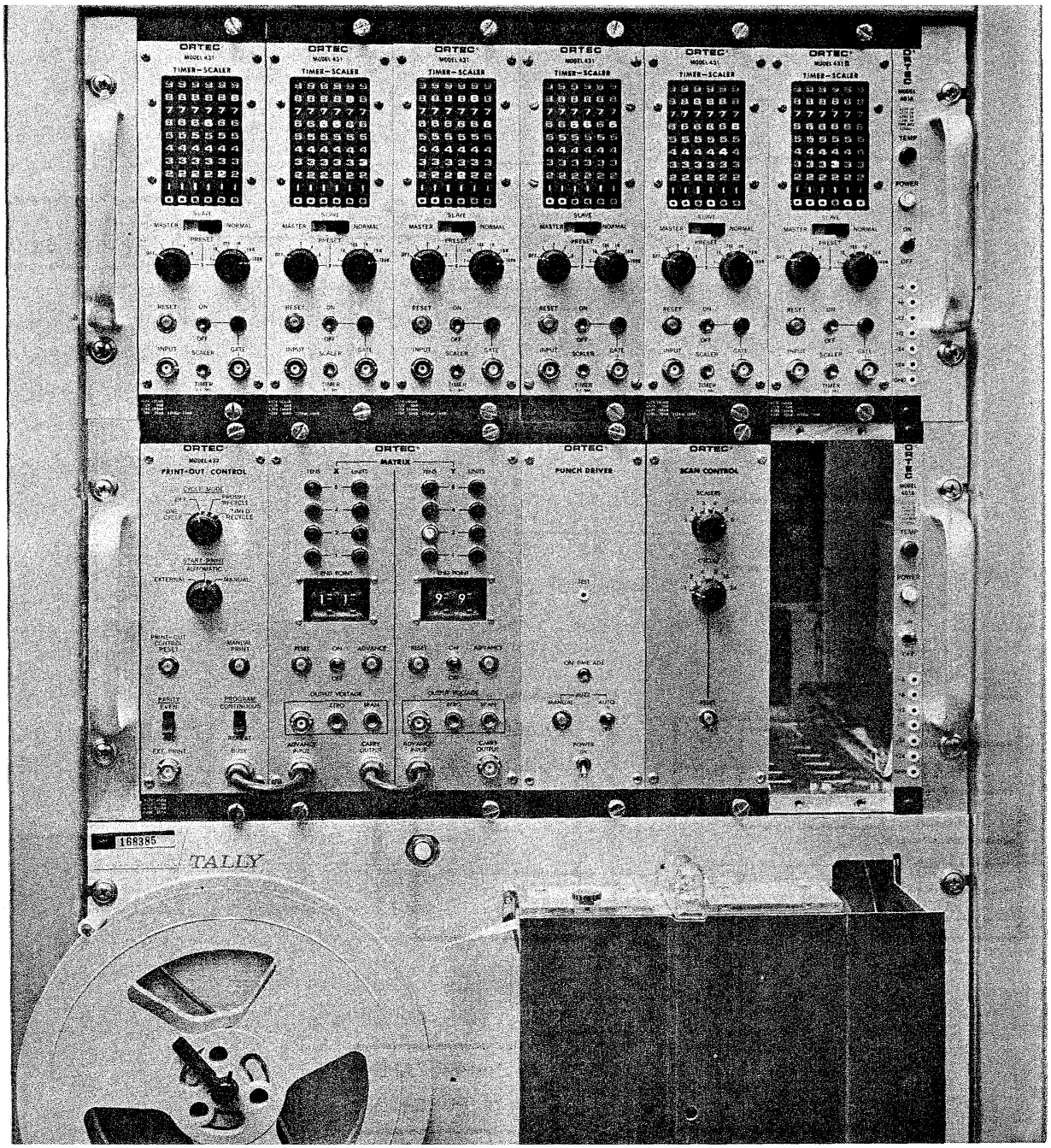

Figure 15. Front view of the matrix scanner.

consider the overall sequence of matrix scanner operation. This operation is summarized in Figure 16.

The analyst first selects a one- or two-dimensional array of points (line or raster) for the problem under investigation. Through the program control unit, he predetermines the dimensions of the array as well as other parameters of the operation. At the start of the analysis, the program control directs the beam positioner to deflect the electron beam to the first position of the preselected array. The timer-scaler block is directed to record the signals produced at the x-ray detectors, as well as beam or monitor current signals, for a fixed time period or until a preset integrated current level is attained. At the end of the counting period, the information accumulated in the scalers and timer is punched on paper tape. After this, the program control resets the timer and scalers, advances the electron beam to the next position in the array, and the counting phase is repeated. All the points of the array are automatically measured in this way. A selection switch on the unit permits automatic repetition of the array a preset number of times.

The matrix scanner is composed of two functional subsystems. The data acquisition components are the print-out control unit, timer, scalers, teletypewriter, punch driver, and paper tape punch, while the matrix generator components are the print-out control, x-y matrix module, and scan control unit. The print-out control, common to both subsystems, functions as an interconnective module for the two subsystems. Each component is compatible with AEC nuclear instrumentation module (NIM) standards and all but three are "stock items" which were available at the time the system was developed. It was necessary for our electronics supplier, ORTEC, Inc.[1],

---

[1]The mention of a supplier is for descriptive purposes only and does not imply recommendation or endorsement by the National Bureau of Standards.

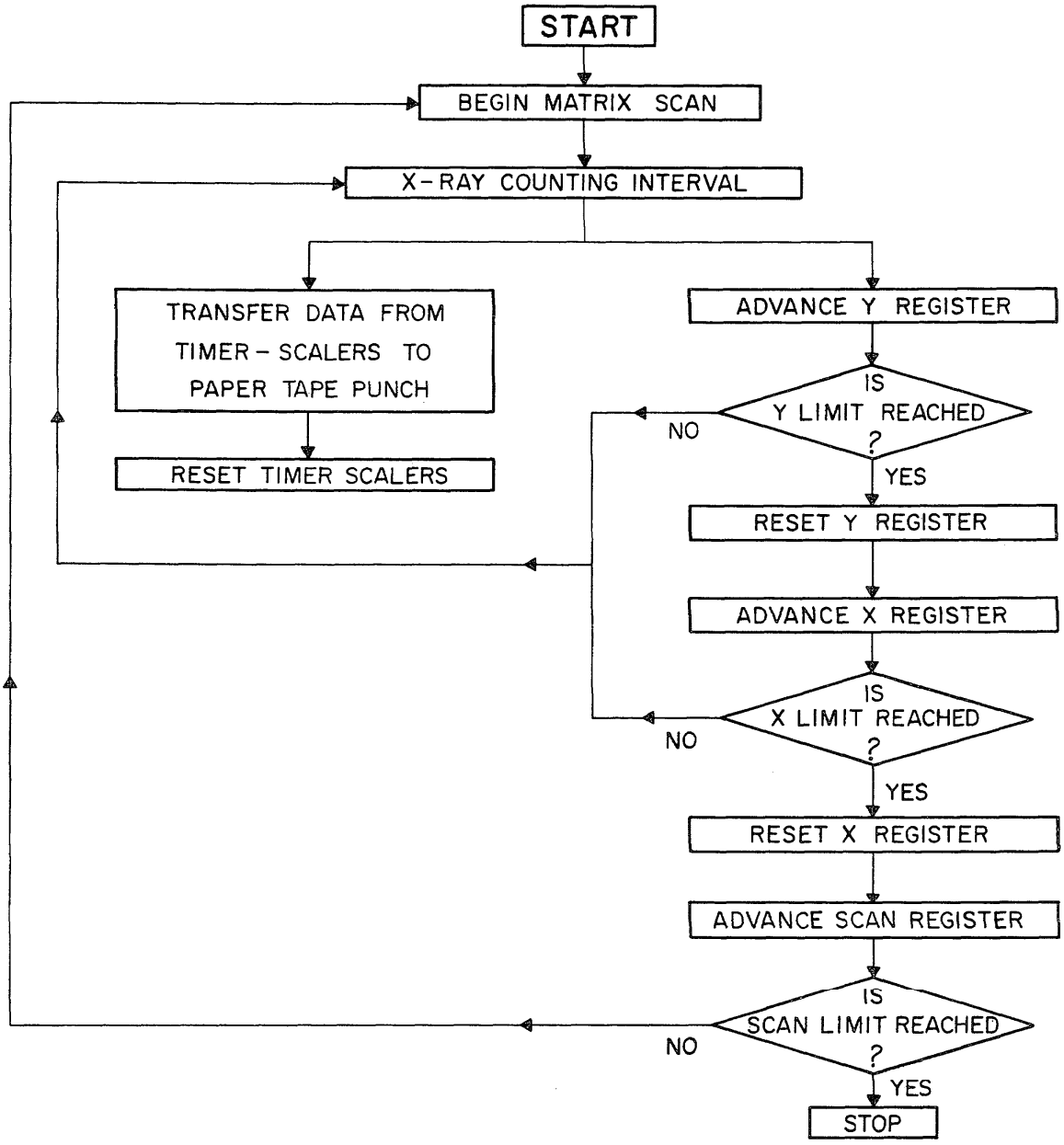

Figure 16. Sequence of automatic operations performed by the matrix scanner.

to especially construct the x-y matrix and scan control units and to modify the print-out control to our specifications.

In the data acquisition subsystem, the print-out control serves as a data scanner to transfer data from the scalers and timer, one character at a time, to the teletypewriter or high-speed paper tape punch. In addition, it resets and restarts the scalers and timer in the proper sequence. A variety of signals, in addition to x-ray counts, can be integrated on the scalers; for example, monitor current or specimen current can be measured with the use of an analog-to-digital converter. When the 60 character/sec paper tape punch (Tally, Model 420) is utilized, a punch driver module is required in order to convert the low-level logic signals of the print-out control to a power level adequate to drive the punch. All tapes, including those produced on the teletypewriter (Teletype, Model 33) are punched in the ASCII code.

In the matrix generator subsystem, the print-out control signals the x-y matrix module to advance to the next location each time the timer reaches its preset limit. The x-y matrix unit generates a one- or two-dimensional matrix of variable size (maximum 100 x 100 locations). The registers of this device advance one y position (column) along a given x (row) after completion of each counting interval. When the preset limit for number of columns is reached, the y-register is returned to the first column and the x-register is advanced to the next row. When the preset row limit is reached, the scan control is checked and execution is stopped if the preset number of scans has been reached; otherwise, both the x and y registers reset to their initial points (0, 0), and the next scan begins. The outputs of the x-y matrix module are dc voltages for x and y, which are proportional to the values of the registers (i.e., location). These voltages are connected to the electron beam scanning system of the electron probe and position the beam to the corresponding

location on the specimen. The distances between measured points on the specimen can be varied over a wide range. In addition to storing the number of scans to be executed, the scan-control unit also stores the number of scalers to be read onto paper tape during each cycle.

Besides micro-homogeneity studies, the matrix scanner can be used in a diversity of applications, including digital wavelength scans, measurement of signal variation as a function of time, and analysis of diffusion couples, inclusions in alloys, and biological specimens. Since, in many cases, information from more than one x-ray channel or other signal channel is available, the correlation of two or more channels may be of interest. Furthermore, the similarity of this procedure with continuous raster scanning suggests that topographic relationships can be investigated. These may include size and shape of single-phase regions, volume fractions occupied by each of the phases, number of inclusions per unit area, variation of composition as a function of distance to grain boundaries, etc. The matrix scanner can thus be used in a wide variety of techniques by selecting the appropriate array and scanning sequence, and by designing computation programs for evaluating the output of this device.

B. Computation Technique

We have written a computer program, named TOPO, to receive data collected with the matrix scanner and to perform the computations essential to the study of micro-homogeneity for binary alloys.

The data for micro-homogeneity studies are x-ray intensities simultaneously measured for two elements at each of the locations in a two-dimensional grid, 10 x 10 locations in this work. We refer to a set of data which contains one measurement for each of the elements at each of the grid locations as one "scan"; several scans may be sequentially

collected on the same grid using the same lines and operating conditions. This yields one "case" consisting of several repetitive scans on a grid.

TOPO performs two major types of computations in analyzing micro-homogeneity. First, statistics are calculated for all the signal intensity data in a case, irrespective of location within the array. These include the mean, square root of the mean, and standard deviation. A frequency distribution of the intensities as a function of distance from the mean is computed and plotted, and, for the sake of comparison, the Poisson distribution with the same mean is presented. Plots of the data are also given in the measurement time sequence, to allow direct observation of time-dependent drifts.

Secondly, intensity variations are displayed as a function of location. The two-dimensional grid is graphically printed on the line printer and the intensity at each location is represented by a symbol indicative of the corresponding range of intensities. This topographical display is very useful in examining the spatial distribution of any micro-homogeneity. As a part of the topographical computation, we have written and included a subroutine for pattern analysis which tests the topograph for the presence of patterns of connected locations having similar intensity levels. This type of analysis is useful not only in homogeneity studies, but also in reducing the data obtained using the matrix scanner in a variety of other modes. Examples of such applications would include studies of diffusion couples, grain boundaries, and micro-inclusions [29]. In the next few paragraphs, we will describe, in somewhat more detail, the operation of TOPO and illustrate its use by selected portions of its printout.

Parameters which specify the number of cases, size of matrix, number of scans, background and pure element intensities, intensity-to-concentration conversion factor, and output options are entered as a set of data cards with each submission of TOPO to the computer. The bulk of the data

(intensities for two elements at each matrix location) is collected on paper tape by the matrix scanner and later transferred to magnetic tape using a paper-to-magnetic tape data converter. The magnetic tape is read by TOPO, one case at a time.

The program TOPO and the 10 user subroutines which it calls (PTLOAD, CHAR, ORTHO, FRAME, GRID, FREDIS, PLOT, PLOT2, PATRN, and RANDOM) were written in Fortran V language for the Univac 1108. The total length of the program and 10 subroutines is about 2000 cards; compilation time is about 15 seconds; and running time for 5 cases is less than 2 minutes. With minor modifications, principally to format statements, fixed-point conversions, and to that portion of the program which loads the data (which are still in a paper tape code) from the magnetic tape, this program can be adapted for use with most Fortran IV compilers on computers having at least 64,000 words of core storage.

At the beginning of processing for each case, PTLOAD is called to load intensities for the given case. The intensities are read from a seven-channel magnetic tape and consequently, are not obtained as a direct image of the original eight-channel paper tape; in the paper-to-magnetic tape conversion, the bits of each paper tape character are divided into two magnetic tape characters. This necessitates bit-by-bit interpretation in PTLOAD, and its internal subroutine CHAR, and restoration of the original data format. Upon completion of this processing, a complete listing of the input data is printed.

Several statistics, including the number of observations, mean, square root of the mean, and standard deviation, are computed and printed for the "raw" intensity data. Also, a frequency distribution of the intensities as a function of distance from the mean and, for the sake of comparison, the Poisson distribution with the same mean are presented as a

table. A graph of the frequency distribution is then displayed in the computer output. Finally, as a graphical test for drift, plots of the intensities in measurement time sequence are included. These computations and graphs are prepared in the subroutines FREDIS, PLOT, and PLOT2.

After the statistics for "raw" intensities are computed, program control is returned to TOPO where data correction and calibration computations are performed. The background correction and dead-time correction are made according to customary methods. The intensities corrected for these two effects are used in a calibration equation to determine the concentration at each location; each element is processed in this way. The general calibration equation is:

$$I_i/I_s = m \cdot C_i/C_s, \qquad (1)$$

where i is a tally of measurements, I_i and C_i are the x-ray intensity concentration at i, I_s and C_s are the x-ray intensity and concentration from a standard, and m is a proportionality constant relating the two ratios. The term m includes calibration for the effects of fluorescence, absorption, and atomic number, and is determined from theory or by empirical means prior to the beginning of the TOPO run. In the application of TOPO, described in the next section of this report, we know the average composition of each specimen; and we used it as the standard. When this technique is employed, we have, for each element, $C_s = \overline{C}$ and $I_s = \overline{I}$, where $\overline{I}$ is the mean x-ray intensity over the entire matrix and $\overline{C}$ is the given mean concentration for the element. In addition, we used the approximation that the two ratios given in equation (1) are directly proportional, i.e., that m=1. When these three substitutions are made in equation (1) and it is solved for C_i, we obtain the calibration equation used in this work:

$$C_i = \overline{C} \cdot I_i/\overline{I}. \qquad (2)$$

The C_i's obtained by equation (2), are next corrected for effects of linear and quadratic terms of drift as a function of measurement sequence time, and the effect of overlapping successive scans on the same specimen array. The effect of each of these terms is expressed as a coefficient, here called a_j, where the subscript j labels the coefficient with respect to the effect it represents. Coefficient a_1 is the mean concentration and if no other effects or biases were present, i.e., the other coefficients were zero, then C_i would be the same as a_1. The coefficients a_2 and a_3 contain the drift effects, while all the remaining a's, one fewer than the total number of scans, express scan-overlap effects. The necessity for corrections of the latter type arises because of the possibility of specimen contamination during electron probe analysis. Such contamination may be increased on successive scans and thereby have a different effect on the measured intensities in each scan after the first. All the a coefficients are determined by substituting the C's obtained in equation (2) into the set of equations:

$$C_i = a_1 + a_2 t_i + a_3 (t_i)^2 + \left(\sum_{j=4}^{n+2} a_j r_{jk} \right) + \delta_i . \qquad (3)$$

In these equations, C and i have the same definition as before, t is measurement sequence time, k is a counter which indexes the scan within which the $i^{\underline{th}}$ measurement is located, r is a switch which indicates the presence of a scan-overlap condition, and δ includes the error from Poisson and non-Poisson sources and, most importantly, any inhomogeneity present at the point. Where n is the number of scans and p is the number of locations per scan, we have as limits for i and mathematical definitions for k and r:

$$1 \leq i \leq np, \qquad (4)$$

$$k = \mathrm{INT}\ (i/p) + 1, \qquad (5)$$

$$r_{jk} = 0 \text{ if } k < j-2, \quad \text{and} \tag{6}$$

$$r_{jk} = 1 \text{ if } k \geq j-2. \tag{7}$$

In equation (5), the function INT computes the closest integer which is less than the argument. The method for determining a's in equation (3) is a conventional least squares regression; in this case, the fit is selected to minimize the sum of the squared values of the deviations in the C's. The regression computation is performed in the subroutine ORTHO. Following these corrections, statistics similar to those computed for the "raw" data are calculated and displayed (See Figure 17 and 18).

When multiple scans are obtained, average C's are calculated for each specimen location. The topographic displays are produced in two ways, relative and absolute. In the relative topograph, local deviations for the mean concentration are displayed by arbitrary symbols using the standard deviation as a scale. Examples of relative topographs appear in Figure 19; the key indicates the scale of deviation from the mean. The range of ± 1 standard deviation is left blank because we are mainly interested in observing which locations lie outside that range. The relative topograph is especially useful for comparing results on elements at two different concentration levels; because the standard deviation is used as the scale unit, all relative topographs have the same approximate coverage in each scale range. Subroutines FRAME and GRID are used in the printout of the relative topographs and the absolute topographs. Absolute topographs show the local deviation in concentration from the mean, using symbols which designate concentration ranges on an absolute scale.

In analysis of micro-homogeneity, the importance of these two types of topographs lies in the fact that they can be examined for patterns (groupings) of locations of similar concentration level. These examinations, which were performed

ELEMENT NUMBER : 2 THE STATISTICS ON THE NEXT FOUR PAGES TREAT FREQ. DIST. VS CUMULATIVE NUMBER BELOW OR =

DRIFT AND OVERLAP CORRECTED INTENSITIES

NUMBER : 100

MEAN : 161191.950

SIGMA : 373.061

SQR RT MEAN: 401.487

K	M+-K*SQR(M)	PCT. BELOW	POISSON	NO. BELOW OR=	PCT. IN INCREMENT	NO. IN INCREMENT
-3.00	159987.4900	.000	.100	0.	.000	0.
-2.66	160121.3200	.000	.400	0.	.000	0.
-2.32	160255.1500	1.000	1.000	1.	1.000	1.
-1.99	160388.9800	2.000	2.300	2.	1.000	1.
-1.66	160522.8000	6.000	4.800	6.	4.000	4.
-1.32	160656.6300	6.000	9.200	6.	.000	0.
-.99	160790.4600	12.000	15.900	12.	6.000	6.
-.66	160924.2900	22.000	25.200	22.	10.000	10.
-.32	161058.1100	39.000	37.100	39.	17.000	17.
.00	161191.9400	50.000	50.000	50.	11.000	11.
.33	161325.7800	60.000	62.900	60.	10.000	10.
.67	161459.6000	76.000	74.800	76.	16.000	16.
1.00	161593.4300	88.000	84.100	88.	12.000	12.
1.33	161727.2600	91.000	90.800	91.	3.000	3.
1.67	161861.0800	95.000	95.200	95.	4.000	4.
2.00	161994.9100	99.000	97.700	99.	4.000	4.
2.33	162128.7400	99.000	99.000	99.	.000	0.
2.67	162262.5700	100.000	99.600	100.	1.000	1.
3.00	162396.3900	100.000	99.900	100.	.000	0.

NUMBER OF ITEMS ABOVE +3*SQR OF MEAN = 0.

Figure 17. Statistics for .6 Au in a .6 Au - .4 Ag binary.

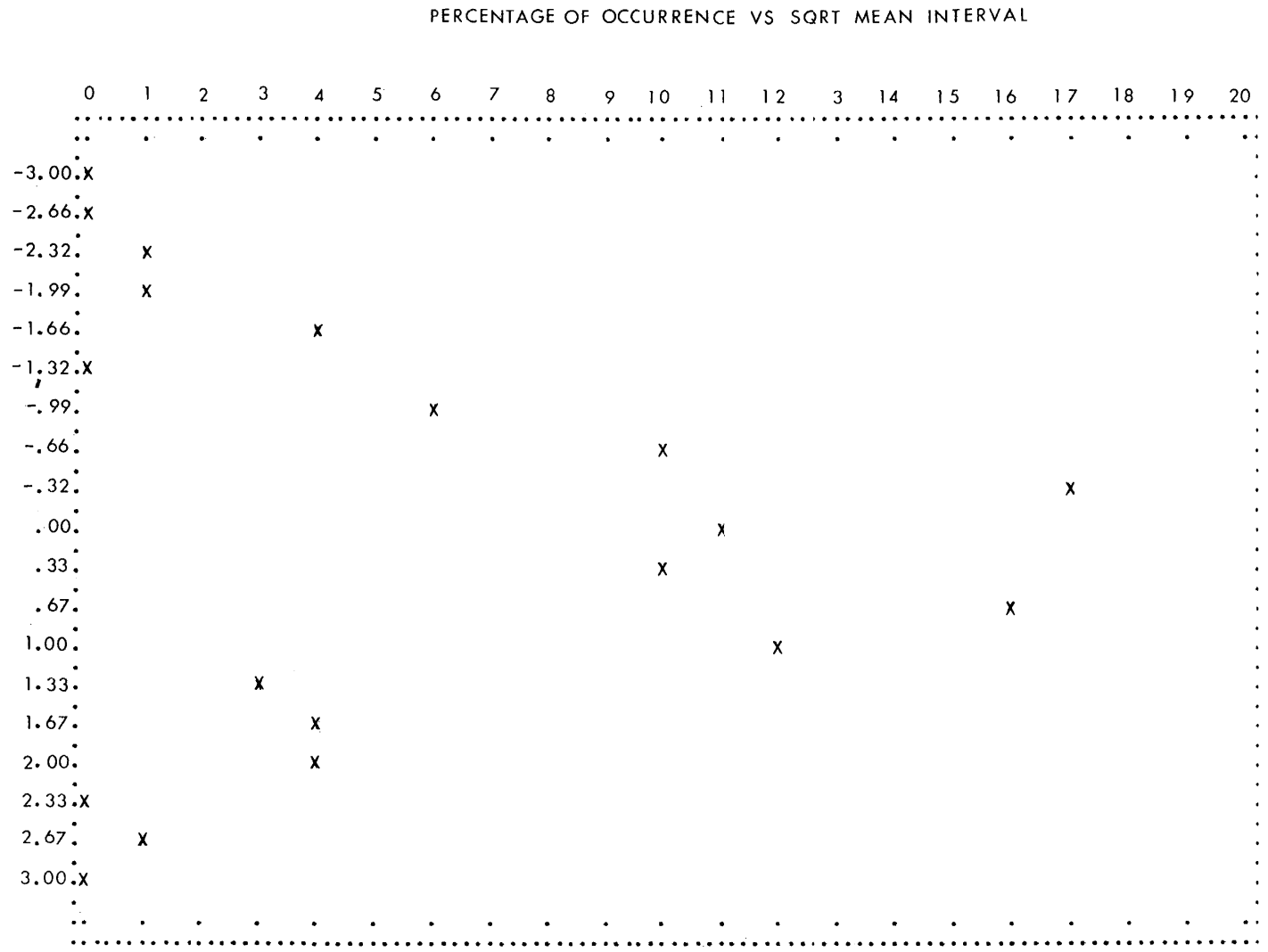

Figure 18. Frequency distribution for the data presented in Figure 17.

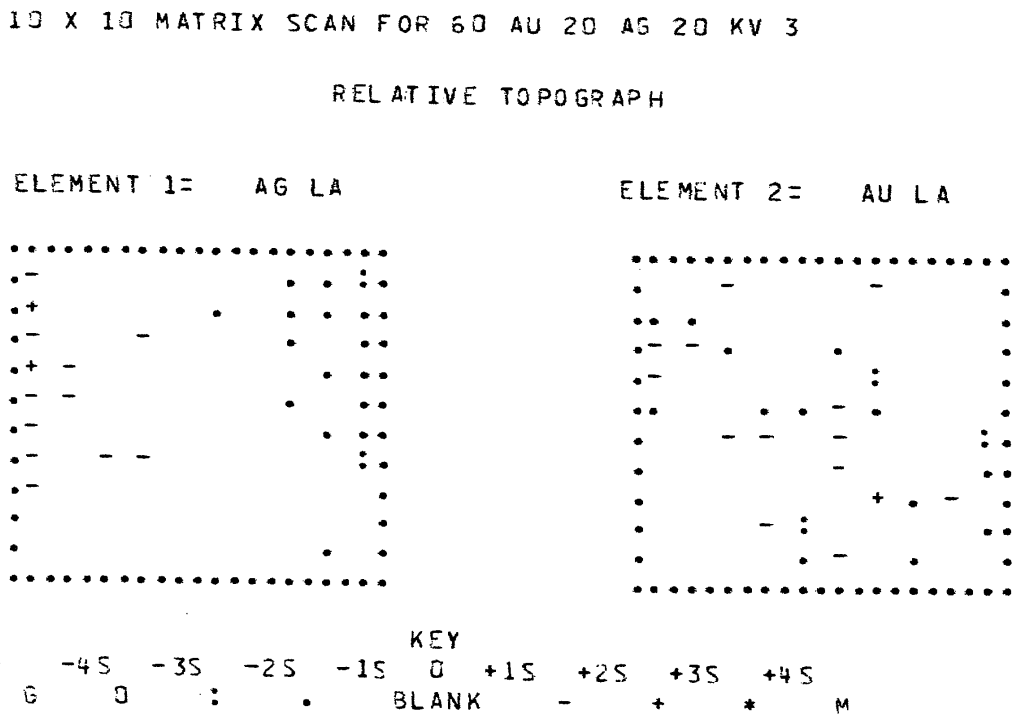

Figure 19. Relative topograph for the case given in Figure 17.

at first by the investigator, can now be done automically by means of a subroutine we call PATRN. PATRN classifies clusters of locations (separating positive from negative in the current version) as to size. Then it determines the total number of clusters within each size class. Cluster size is not simply defined as the number of locations connected in a cluster, but is weighted as a function of the "compactness" of the cluster. This is done by counting the links (diagonal links are included) between the locations in a cluster (See Figure 20). Entrance to the first location of a cluster is counted as a link so that single points will be of size 1.

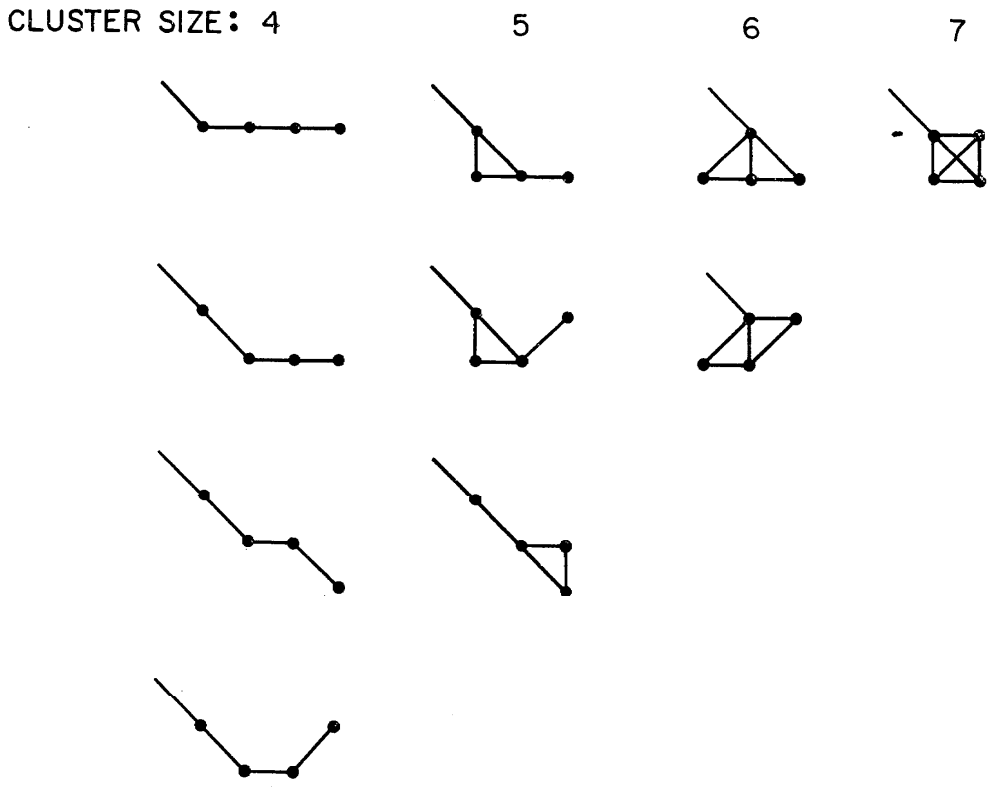

Figure 20. Method of defining cluster size by counting links. Note extra weight given for "compactness."

A part of PATRN is designed to show if the amount of structure observed differs from that which would, with significant probability, randomly occur. To make this test, we scramble the array. The resulting pattern is analyzed and then the random-assignment process is repeated, again followed by analysis. The complete operation of random-assignment and analysis is repeated until 10 random patterns have been evaluated. This information can then be compared with that obtained directly from the observed pattern (See Figure 21).

P A T T E R N A N A L Y S I S
O F L I N K S

NON-RANDOMIZED

ELEMENT 1				ELEMENT 2			
POS.		NEG.		POS.		NEG.	
SIZE	NO.	SIZE	NO.	SIZE	NO.	SIZE	NO.
13		17		14		16	
1	1	1	2	1	5	1	4
2	1	2	0	2	1	2	3
3	0	3	0	3	0	3	2
4	0	4	0	4	2	4	0
15	1	15	0	15	0	15	0
29	0	29	1	29	0	29	0

P A T T E R N A N A L Y S I S
O F L I N K S

MONTE CARLO DISTRIBUTION (10 SETS)

ELEMENT 1				ELEMENT 2			
POS.		NEG.		POS.		NEG.	
SIZE	NO.	SIZE	NO.	SIZE	NO.	SIZE	NO.
1	10.40	1	9.80	1	9.40	1	8.80
2	4.10	2	3.20	2	3.60	2	3.60
3	.90	3	1.20	3	.40	3	1.90
4	1.00	4	.80	4	.90	4	.70
5	.50	5	.40	5	.30	5	.60
6	.00	6	.40	6	.70	6	.10
7	.20	7	.10	7	.10	7	.00
8	.10	8	.00	8	.00	8	.20
9	.00	9	.10	9	.20	9	.00
10	.10	10	.10	10	.00	10	.10
11	.10	11	.20	11	.00	11	.00
13	.10	13	.00	13	.00	13	.00

8723704934

Figure 21. Pattern analysis for the relative topograph in Figure 19. Notice that a strong pattern is indicated for element 1 (Ag), while the analysis for element 2 (Au) shows a lack of clustering; i.e., structures similar to those found are likely to occur by chance.

We now introduce two other topographs which show sum and difference correlations. In the case of the sum correlation topograph, the algebraic sum of the two absolute topographs is computed and displayed on a point-by-point basis. Similarly, for the difference correlation topograph, the algebraic difference of the two absolute topographs is computed and displayed on a point-by-point basis. In a binary alloy, any increase in the concentration of one element at a point must be accompanied by a decrease in the second element at the same point. If this correlation is not observed, i.e., if both elements decrease, or if one decreases with no change observed for the second, the presence of a third element may be indicated. This is not a certain result because the changes could be caused by instrumental difficulties. Instrumental problems are certainly suspect if both elements increase at a given location.

An alternative method for examining these correlations is show in Figure 22. Here the departure from the mean at each location is plotted for both elements along orthogonal axes. Figure 23 illustrates several of the possible outcomes for such plots. A nearly circular grouping centered on the origin indicates a homogeneous binary alloy and measurements of equal precision for both elements. Elliptically shaped scatter about either of the axes means the precision was poorer for the element plotted on that axis. Negative correlation, that is, an increase in one element when the other decreases, is a condition necessary for concluding that inhomogeneity is observed. Positive correlation results when experimental errors are common to both elements and affect them in the same direction (e.g., short duration beam intensity fluctuation).

10 X 10 MATRIX SCAN FOR 60 AU 20 AG 20 KV 3

CORRELATION GRAPH

ELEMENT 1 IS PLOTTED ON THE ORDINATE (VERT) AND ELEMENT 2 IS PLOTTED ON THE ABSCISSA (HORZ).
FOR EACH AXIS THE SCALE IS FROM -1.5% TO +1.5%.

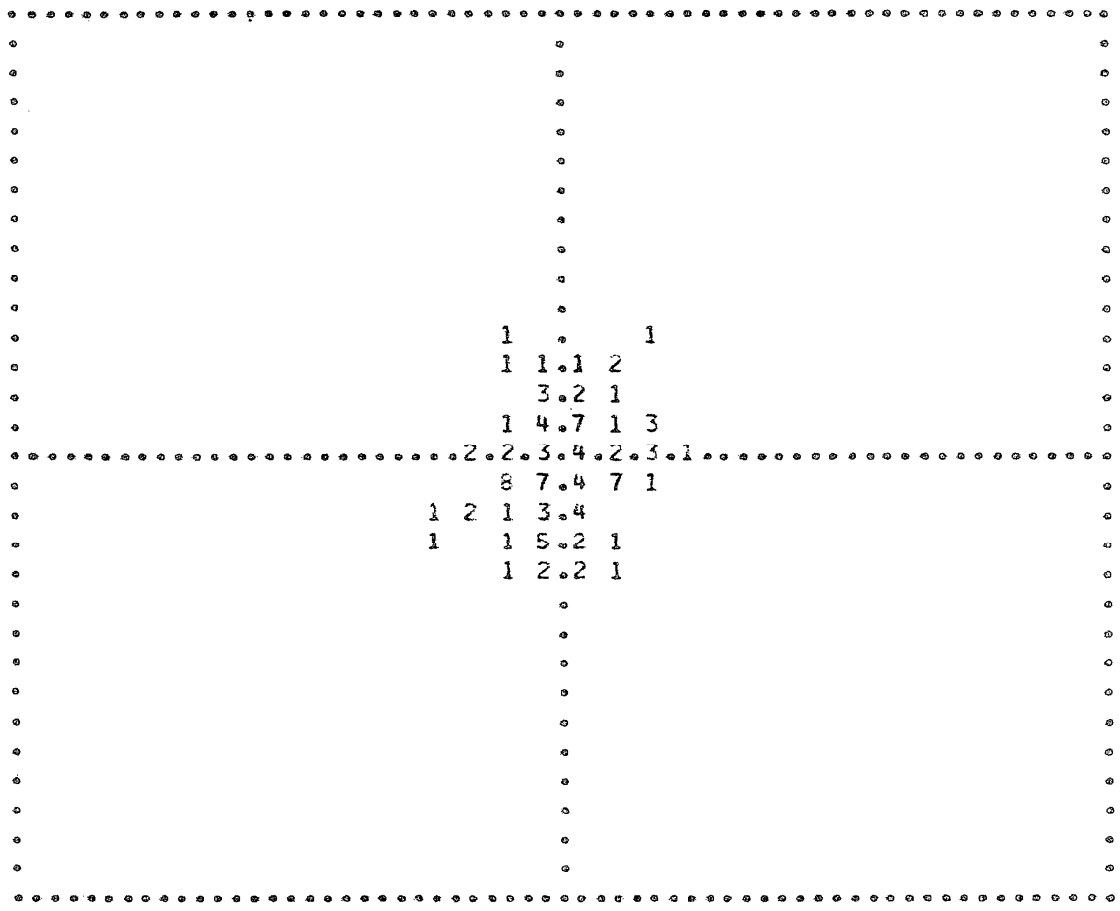

Figure 22. Correlation graph for the case given in Figure 17. Deviations from the mean Ag concentration are plotted on the ordinate while the deviations from the mean Au concentration are plotted on the abscissa. Deviations for neither element exceed 0.004, indicating good homogeneity.

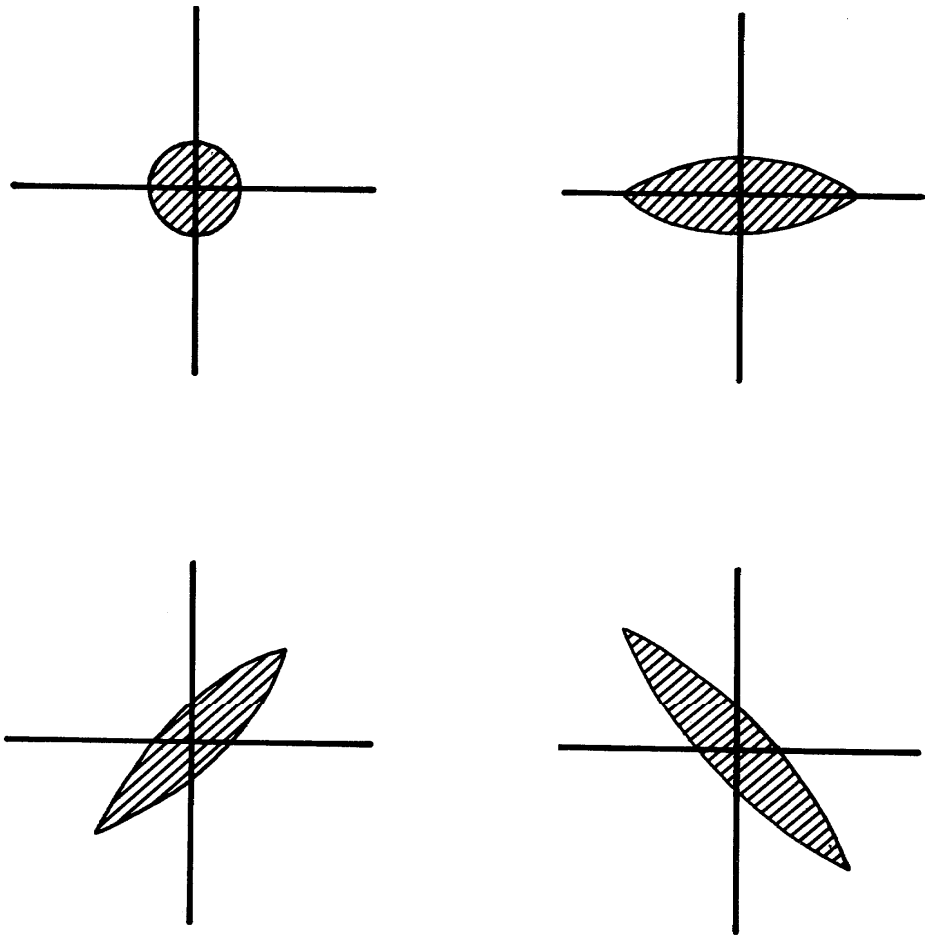

Figure 23. Four possible outcomes for the correlation graphs. The conditions indicated by these graphs are described in the text.

FORM NBS-114A (1-71)

U.S. DEPT. OF COMM. BIBLIOGRAPHIC DATA SHEET	1. PUBLICATION OR REPORT NO. NBS-SP-260-28	2. Gov't Accession No.	3. Recipient's Accession No.

4. TITLE AND SUBTITLE Standard Reference Materials: Preparation and Evaluation of SRM's 481 and 482 Gold-Silver and Gold-Copper Alloys for Microanalysis

5. Publication Date: August 1971

6. Performing Organization Code

7. AUTHOR(S) Kurt F. J. Heinrich, Robert L. Myklebust, Stnaley D. Rasberry, and Robert E. Michaelis

8. Performing Organization

9. PERFORMING ORGANIZATION NAME AND ADDRESS

NATIONAL BUREAU OF STANDARDS
DEPARTMENT OF COMMERCE
WASHINGTON, D.C. 20234

10. Project/Task/Work Unit No. 310 2127

11. Contract/Grant No.

12. Sponsoring Organization Name and Address

13. Type of Report & Period Covered: Final 1968-1971

14. Sponsoring Agency Code

15. SUPPLEMENTARY NOTES

16. ABSTRACT (A 200-word or less factual summary of most significant information. If document includes a significant bibliography or literature survey, mention it here.)

The reasoning behind the choice of the systems Au-Ag and Au-Cu for SRM's, and their suggested uses are described. We also report on the preparations of the materials, their chemical analysis, the tests performed to ascertain macroscopic and microscopic homogeneity, and on relative x-ray intensity measurements at various x-ray lines and voltages. A description of the instrumentation (matrix scanner), techniques, and programs employed in the homogeneity studies, as well as tables and graphs of the x-ray intensity measurements, are appended.

17. KEY WORDS (Alphabetical order, separated by semicolons)

Alloys; corrections; electron probe; homogeneity; matrix scanner; microanalysis; quantitative analysis; standard reference materials; x-ray emission.

18. AVAILABILITY STATEMENT

[XX] UNLIMITED.

[ ] FOR OFFICIAL DISTRIBUTION. DO NOT RELEASE TO NTIS.

19. SECURITY CLASS (THIS REPORT)	21. NO. OF PAGES
UNCLASSIFIED	100
20. SECURITY CLASS (THIS PAGE)	22. Price
UNCLASSIFIED	$1.00

USCOMM-DC 66244-P71